Dynamics and efficiency of a self-propelled, diffusiophoretic swimmer

Benedikt Sabass[1] and Udo Seifert[1]
II. Institut für Theoretische Physik, Universität Stuttgart, 70550 Stuttgart, Germany

Active diffusiophoresis - swimming through interaction with a self-generated, neutral, solute gradient - is a paradigm for autonomous motion at the micrometer scale. We study this propulsion mechanism within a linear response theory. Firstly, we consider several aspects relating to the dynamics of the swimming particle. We extend established analytical formulae to describe small swimmers, which interact with their environment on a finite lengthscale. Solute convection is also taken into account. Modeling of the chemical reaction reveals a coupling between the angular distribution of reactivity on the swimmer and the concentration field. This effect, which we term "reaction induced concentration distortion", strongly influences the particle speed. Building on these insights, we employ irreversible, linear thermodynamics to formulate an energy balance. This approach highlights the importance of solute convection for a consistent treatment of the energetics. The efficiency of swimming is calculated numerically and approximated analytically. Finally, we define an efficiency of transport for swimmers which are moving in random directions. It is shown that this efficiency scales as the inverse of the macroscopic distance over which transport is to occur.

PACS numbers: 87.15.Vv, 81.16.Hc, 05.70.Ln

I. INTRODUCTION

Active motion, driven by an inhomogeneous chemical surface reaction, has recently attracted much scientific interest. A number of different systems, employing this propulsive mechanism on the micro- and nanometer scale, have been suggested[1–8]. They open exiting, possible routes for future engineering of nano-devices[9–15]. Furthermore, self-propelled small swimmers provide a unique chance to study artificial motion at the nanometer scale, e.g., to investigate anomalous diffusion[16–18] or non equilibrium thermodynamics[19,20]. Other interesting questions relating to mutual interactions of these swimmers and interactions with the environment are also beginning to be addressed[21–24].

In most of these experiments, a catalytic decomposition of hydrogen peroxide H_2O_2 into oxygen $O_2\,(g)$ and water is employed for propulsion. In general, these (electro) chemical processes obey quite nontrivial kinetics[25]. Experiments with bimetallic nanorods, combining two different metallic catalysts, have shown that the mechanism for electrokinetic decomposition of H_2O_2 involves an electrical current inside the particle[5,26]. Theoretical interpretations of these experiments in terms of a phoretic propulsion mechanism have recently emerged[27–29]. They include driving through an interaction of the swimmer with a concentration gradient (diffusiophoresis[30]) as well as driving through interaction with a self-generated charge gradient (self-electrophoresis). Other possible driving mechanisms like interfacial tension gradients[31] and nano-bubble formation[32] have also been investigated. For a different kind of experiment[33] polystyrene particles, half coated with platinum as a catalyst, have been employed. No electric current inside the swimmer is expected here. Michaelis-Menten-like kinetics for the chemical reaction were demonstrated and the data can be consistently explained by a generic diffusiophoretic/self-electrophoretic model[4].

Although the understanding of phoretic driving mechanisms has reached an appreciable level, there remain open questions concerning swimming with progressive miniaturization of the swimming particle. One such question is, how swimming speed changes if the particle size approaches the lengthscale of solute-swimmer interactions. Further challenges concern a more detailed, theoretical modelling of the chemical surface reaction and the solute convection. Both factors can contribute to modified predictions for the swimming behavior. All these issues may also be relevant in terms of optimization for future applications (see citations above).
Finally, the energy balance of the driving mechanism and its efficiency have only received limited attention. Early experimental estimates[3] suggest that the efficiency of bimetallic nanorods is very low (on the order of 10^{-9}). Here the swimming speed was found to be about $1\ldots10\,\mu m/s$. Molecular dynamics simulations of a swimmer in gaseous environment[34] yielded much higher efficiencies of the order 10^{-4} and speeds in the order of m/s . The discrepancy emphasizes the importance of the hydrodynamic dissipation for the efficiency. This point found particular emphasize in our previous theoretical work were we have examined the hydrodynamic efficiency for generic surface driven swimmers[35]. The hydrodynamic efficiency provides an upper bound on the overall efficiency while it does not include dissipative effects related to building up the chemical gradient driving the swimmer. It is a remarkable property of active phoresis that the overall efficiency is fully amenable to theoretical calculations. This contrasts with other active swimming mechanisms,e.g., beating flagella[36], where some microscopic, mechanical degrees of freedom are unknown. Nevertheless, the overall efficiency of a model for active, phoretic swimming in a viscous medium has not yet been calculated. In the present publication we address the above mentioned issues concerning the dynamics and efficiency within a linear response theory employing the established theoretical framework of neutral

diffusiophoresis[30].

This article is organized as follows. In Sec. II, we introduce the model system and the pertaining equations. These are non-dimensionalized and linearized in Sec. III. In Sec. IV, we calculate the speed of the swimmer and analyze its dependence on the interaction between solute and swimmer. The dependence of the swimming speed on the chemical surface reaction is investigated in Sec. V. In Sec. VI, we focus on the energetics of active diffusiophoresis. Here, the efficiency of swimming is analyzed in detail and we also consider a measure for the efficiency of transport.

II. MODEL DESCRIPTION

To explore generic features of active diffusiophoresis, we employ an idealized hydrodynamic model. The swimmer, a spherical particle with radius R, is placed in an infinitely large container. We assume axial symmetry and use a spherical coordinate system aligned in the $\hat{\mathbf{e}}_z$ direction. $\tilde{r}$ is the distance from the particle center and θ is the polar angle with $0 \leq \theta \leq \pi$. The unit vectors of the spherical system are denoted by $\hat{\mathbf{e}}_r$, $\hat{\mathbf{e}}_\theta$. Throughout this publication, we will designate dimensional variables with a tilde ($\tilde{}$), while constants and non-dimensional quantities carry no tilde. The multi-component fluid surrounding the swimmer is assumed to be incompressible and Newtonian. It contains two dilute (non-interacting) solutes, whose molecular volumes and masses are to be similar to that of the solvent. The concentrations of the solutes are denoted by $\tilde{c}_a$ and $\tilde{c}_b$. Solutes and solvent are bound to interact with the surface of the swimming particle, e.g., through van der Waals, electrostatic or steric interactions. In order to simplify the situation, we assume that a common surface potential mediates the interactions between both, the solutes, the solvent and the swimmer. Within our mean-field framework, the common interaction between swimmer and all fluid constituents merely modifies the pressure of the fluid. Only for species b, we assume, on top of this, a radially symmetric potential $\tilde{\Psi}$. Physically, this second potential could, e.g., represent a different polarizability of the solutes b. It is assumed to decay over a characteristic lengthscale L. A similar approach has been taken in a molecular dynamics simulation of the system[6]. In Appendix A we provide a simple physical model of the three-component solution considered in the present publication. Both molecular species, type a and b, have the same diffusion constant D. The concentration fluxes $\tilde{\mathbf{J}}_{\{a,b\}}$ and the corresponding solute conservation laws are

$$\tilde{\mathbf{J}}_a \equiv \tilde{c}_a\tilde{\mathbf{v}} + \tilde{\mathbf{j}}_a = \tilde{c}_a\tilde{\mathbf{v}} - D\nabla\tilde{c}_a, \tag{1}$$

$$\tilde{\mathbf{J}}_b \equiv \tilde{c}_b\tilde{\mathbf{v}} + \tilde{\mathbf{j}}_b = \tilde{c}_b\tilde{\mathbf{v}} - D\left(\nabla\tilde{c}_b + \frac{\tilde{c}_b}{kT}\nabla\tilde{\Psi}\right), \tag{2}$$

$$0 = \nabla\cdot\tilde{\mathbf{J}}_{\{a,b\}}. \tag{3}$$

The diffusive fluxes of solutes relative to the center of mass are denoted by $\tilde{\mathbf{j}}_{\{a,b\}}$. The center of mass fluid velocity that convects the solutes is denoted by $\tilde{\mathbf{v}}$. We assume here that the diffusion of solutes near the surface is similar to the bulk diffusion. An extra surface diffusion term is not taken into account. Generic boundary conditions, allowing for an absorption and emission of solutes at the swimmer's surface, are

$$\begin{aligned}\hat{\mathbf{e}}_r\tilde{\mathbf{J}}_{\{a,b\}}(R,\theta) &= \tilde{\alpha}_{\{a,b\}}\, g(\theta),\\ \nabla\tilde{c}_{\{a,b\}}(\infty,\theta) &= 0.\end{aligned} \tag{4}$$

Here all the θ-dependence of the flux at the surface is contained in the dimensionless function $g(\theta)$. We will always assume that the emission of solutes happens in a spatially asymmetric way. $\tilde{\alpha}_{\{a,b\}}$ has the dimensions of solute flux and quantifies its magnitude. The Stokes equation and incompressibility condition read

$$\eta\nabla^2\tilde{\mathbf{v}} - \nabla\tilde{p} = \nabla\cdot\tilde{\sigma} = \tilde{c}_b\nabla\tilde{\Psi} \quad \text{and} \quad \nabla\cdot\tilde{\mathbf{v}} = 0. \tag{5}$$

Here η is the viscosity of the fluid, which we assume to be spatially constant. The pressure accounting for the incompressibility of the fluid is denoted by $\tilde{p}$ and

$$\tilde{\sigma} \equiv \eta\left(\nabla\tilde{\mathbf{v}} + (\nabla\tilde{\mathbf{v}})^T\right) - \tilde{p}\mathbf{I} = 2\eta\tilde{\mathbf{E}} - \tilde{p}\mathbf{I} \tag{6}$$

is the hydrodynamic stress tensor. In order to make sure that the total force on the fluid is, even for a linear concentration gradient ($\tilde{c}_b \sim \tilde{r}\cos\theta$), convergent we assume

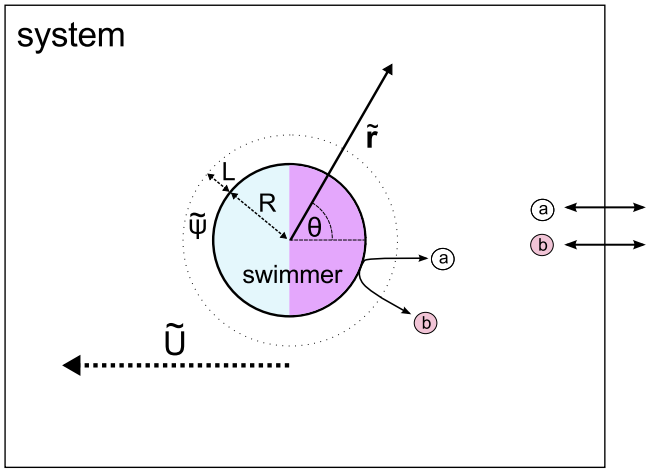

FIG. 1. Schematic representation of the model for an active swimmer. Molecules of type a and b are dissolved in the fluid surrounding the swimmer with radius R. The molecules are transformed into each other through chemical surface reactions and the overall concentrations are maintained constant. An interaction between the swimmer and the type b molecules occurs through the potential $\tilde{\Psi}$, whose lengthscale is given by L. An inhomogeneous distribution of solutes causes the swimmer to move with the speed $\tilde{U}$. $\tilde{\mathbf{r}}$ is the position vector and θ is the polar angle in a spherical coordinate system used throughout.

in the following

$$\tilde{\Psi}\left(\tilde{r}\to\infty\right) < O\left(\frac{1}{\tilde{r}^3}\right). \tag{7}$$

The swimming speed is given by $\tilde{U}$ in the laboratory frame. In the frame moving with the center of the swimmer, it enters the solution of the Stokes equation through the boundary conditions

$$\begin{aligned}\tilde{\mathbf{v}}(\infty,\theta) &= -\tilde{U}\hat{\mathbf{e}}_z,\\ \tilde{\mathbf{v}}(R,\theta) &= 0.\end{aligned} \tag{8}$$

The swimming speed $\tilde{U}$ is determined from the balance of forces acting on the swimmer in the overdamped limit

$$0 = \tilde{F}_{\mathrm{m}}\hat{\mathbf{e}}_z + \int \tilde{c}_b\nabla\tilde{\Psi}\mathrm{d}\tilde{V} + \int \tilde{\sigma}\hat{\mathbf{e}}_r\mathrm{d}\tilde{A}_{\tilde{r}=R}. \tag{9}$$

Since the swimmer is spherical, we can identify the normal vector on the surface of the sphere with the unit radial vector $\hat{\mathbf{e}}_r$. We are considering a freely moving swimmer, therefore the external force $\tilde{F}_{\mathrm{m}}$ will be set to zero. The dependence of $\tilde{\sigma}$ on $\tilde{U}$ allows the calcuation of the latter quantity from Eq. (9). In a perturbative approach for small $\tilde{\Psi}/kT$, one can assume that the body force $\nabla\cdot\tilde{\sigma} = \tilde{c}_b\nabla\tilde{\Psi}$ is independent of the fluid velocity $\tilde{\mathbf{v}}$. Due to the linearity of the Stokes equation Eq. (9) can be reformulated employing a reciprocal relation[37]. The result for spherical swimmers is

$$\begin{aligned}0 = \tilde{F}_{\mathrm{m}} - 6\pi\eta R\tilde{U} - \int[&(\frac{3R}{2\tilde{r}} - \frac{R^3}{2\tilde{r}^3} - 1)\cos\theta\,\hat{\mathbf{e}}_r\nabla\cdot\tilde{\sigma}\\ &-(\frac{3R}{4\tilde{r}} + \frac{R^3}{4\tilde{r}^3} - 1)\sin\theta\,\hat{\mathbf{e}}_\theta\nabla\cdot\tilde{\sigma}]\mathrm{d}\tilde{V}.\end{aligned} \tag{10}$$

However, when convection strongly modifies the solute distribution $\tilde{c}_b$, Eq. (10) does not permit to calculate $\tilde{U}$.

The swimmer model presented above is only valid if the assumption of a dilute solution holds. Corrections to the diffusion coefficient, resulting from mutual solute-solute interactions, are proportional to the volume fraction and we hence demand $\tilde{c}_{\{a,b\}}\,a^3 \ll 1$ for solutes with radius a. Another source of error is introduced by the rotational diffusion of the swimmer. The rotating frame results in a corrective term for the solute fluxes Eq. (1,2) of the form $-\hat{\mathbf{e}}_\theta\tilde{r}\,D_{\mathrm{rot}}\,\partial_\theta\tilde{c}_{\{\mathrm{a,b}\}}$ where D_{rot} is the rotational diffusion coefficient of the swimmer. The relative magnitude of this correction for the diffusion equations (1-3) is of the order R^2D_{rot}/D. Employing the Einstein relations for the diffusion coefficients $D = kT/\left(6\pi\eta a\right)$, $D_{\mathrm{rot}} = kT/\left(8\pi\eta R^3\right)$, we have $R^2D_{\mathrm{rot}}/D = 3a/(4R)$. Accordingly, we demand in the following $a \ll R$. This assumption also justifies disregarding hydrodynamic corrections of the solute-swimmer interaction due to the finite size of the solutes. Taken together, our model is restricted to swimmers which are at least two magnitudes larger than the solutes. If the solute radii are in the Å range, we hence require $R \gtrsim 30\,\mathrm{nm}$.

III. THE LINEARIZED, NON-DIMENSIONAL EQUATIONS

Convective transport renders the diffusion equations (1-3) nonlinear since the fluid velocity and the concentration fields are both unknown. The fluid velocity $\tilde{\mathbf{v}}$ is determined by Eq. (5) and thus depends itself on $\tilde{c}_b$. In order to make the system more amenable to analytic calculations we linearize the non-dimensionalized equations around equilibrium. We thereby construct a linear response theory for active diffusiophoresis. The natural length- and energy scales are the radius of the swimmer, R, and the thermal energy kT. Accordingly, we rescale as $r \equiv \tilde{r}/R$ and $\Psi \equiv \tilde{\Psi}/kT$. The intrinsic lengthscale L of the potential Ψ is denoted in dimensionless form as

$$\lambda \equiv L/R. \tag{11}$$

Particle swimming is driven by an asymmetric concentration perturbation of the equilibrium distribution of b-type solutes $\tilde{c}_b^{\mathrm{eq}}(\tilde{r})$. Owing to the radial symmetry of $\tilde{\Psi}$, only the dipole moment of the concentration perturbation

$$\frac{3}{2}\int_{-1}^{1}\frac{R\,\tilde{\alpha}_b}{D}\,g(\theta)\,\cos\theta\,\mathrm{d}(\cos\theta) \tag{12}$$

contributes here. We can accordingly define the concentration scale $\hat{c}$, which is relevant for the particle motion, as

$$\hat{c} \equiv R\,\tilde{\alpha}_b/D. \tag{13}$$

In the following we will always assume that the concentration perturbation $\hat{c}$ is much smaller than the equilibrium concentration scale. We can then define a new dimensionless parameter as

$$\delta \equiv \hat{c}/\tilde{c}_b^{\mathrm{eq}}(\infty). \tag{14}$$

Throughout this publication, we employ $\hat{c}$ for the non-dimensionalization of concentrations. The equilibrium perturbations of the concentration fields are

$$c_a \equiv \frac{\tilde{c}_a - \tilde{c}_a^{\mathrm{eq}}(\infty)}{\hat{c}}, \tag{15}$$

$$c_b \equiv \frac{\tilde{c}_b - \tilde{c}_b^{\mathrm{eq}}(\infty)e^{-\Psi}}{\hat{c}}. \tag{16}$$

The solute fluxes $\tilde{\mathbf{j}}$ are non-dimensionalizd by $D\hat{c}/R$ and obey the boundary conditions

$$\hat{\mathbf{e}}_r\mathbf{j}_{\{a,b\}}(1,\theta) = \frac{R\,\tilde{\alpha}_{\{a,b\}}\,g(\theta)}{D\hat{c}} \equiv \alpha_{\{a,b\}}g(\theta). \tag{17}$$

A typical diffusiophoretic speed magnitude[30] is given for $\lambda \lesssim 1$ by

$$\hat{U} \equiv \frac{kT\,L^2}{\eta}\frac{\hat{c}}{R}. \tag{18}$$

We define an associated Peclét number by

$$\mathrm{Pe} \equiv \frac{\hat{U} R}{D}. \tag{19}$$

Sample calculations, employing measured particle speeds[26,33], show that Pe is typically small, on the order of 10^{-2}. The Peclét number thus constitutes, besides δ, a second small expansion parameter. Employing the non-dimensional hydrodynamic variables $\mathbf{v} \equiv \tilde{\mathbf{v}}/\hat{U}$ and $p \equiv \tilde{p} R/(\hat{U}\eta)$, the equations for solute conservation (1-3) and the Stokes equation (5) become

$$\nabla^2 c_b + \nabla \cdot (c_b \nabla \Psi) - \frac{\mathrm{Pe}}{\delta} \mathbf{v} \nabla e^{-\Psi} = \mathrm{Pe}\, \mathbf{v} \nabla c_b, \tag{20}$$

$$\nabla^2 c_a = \mathrm{Pe}\, \mathbf{v} \nabla c_a, \tag{21}$$

$$\nabla^2 \mathbf{v} - \nabla p - \frac{1}{\lambda^2} c_b \nabla \Psi = 0. \tag{22}$$

The fluid boundary conditions are, as before,

$$\begin{aligned} \mathbf{v}(\infty, \theta) &= -U \hat{\mathbf{e}}_z, \\ \mathbf{v}(1, \theta) &= 0. \end{aligned} \tag{23}$$

The form of Eqns. (20,21) suggests a perturbation scheme in Pe to cope with the nonlinearities. However, difficulties arise if δ is of the same magnitude as Pe . Then only the right hand sides of Eqns. (20,21) are small. Furthermore, because $\delta \sim \hat{c}$ and also $\mathrm{Pe} \sim \hat{c}$, it is in the spirit of a linear response theory in $\hat{c}$ to set

$$\mathrm{Pe}\, \mathbf{v} \nabla c_a \simeq \mathrm{Pe}\, \mathbf{v} \nabla c_b \simeq 0. \tag{24}$$

This linearization approach has the merit that the mobility of the swimmer, relating U to $\alpha_{\{a,b\}}$, can be calculated straightforwardly. To do this, one only needs to determine the force balance Eq. (9) for the two cases $\alpha_{\{a,b\}} = 0$ and $U = 0$. This procedure was described in detail by O'Brien and White[38]. For concrete numerical and analytical calculations we always rewrite the Stokes equation (22) by employing the stream function formalism[39].

The approximation Eq. (24) does not go without any caveat. The convection terms dominate the diffusion terms in Eqns. (20,21) for large r due to different orders of radial derivatives. In general, one would therefore follow Acrivos and Taylor[40] and split the solution for the concentration field into an inner solution, with coordinate r, where diffusion dominates and an outer solution, with rescaled radial coordinate $\mathrm{Pe}\, r$, where convection dominates. We avoid this procedure by assuming that $\lambda\, \mathrm{Pe} \ll 1$. Then the interaction between solutes and swimmers takes place in the diffusion-dominated region around the swimmer.

In contrast to the approach taken here, the standard way to make analytical progress in view of the difficulties inherent in Eqns. (1-5) is to assume that the magnitude of the surface potential is small ($\Psi(1) \ll 1$). Then convection does not occur in the $O\left(\Psi(1)^1\right)$ contribution of a regular perturbation scheme. The resulting "Debye-Hueckel" -like theory is practical in the case of ionic surface interactions[41] but may become inappropriate for non-ionic interactions when $\Psi(1)$ is not small.

IV. SWIMMING SPEED AND THE ROLE OF THE INTERACTION POTENTIAL

The nature of the potential Ψ, comprising a variety of possible physical interactions, is important for the diffusiophoretic speed. In order to demonstrate this in this section, we leave here all issues concerning the details of the chemical reactions aside. This simplification also facilitates a comparison with other work[4,33]. The emission rate of the solute of type b is in this section given by $g(\theta) = (1 + \cos\theta)$ and $\tilde{\alpha}_b = \kappa = \mathrm{const}$. We then have

$$\hat{\mathbf{e}}_r \tilde{\mathbf{j}}_b(\theta) = \kappa\, (1 + \cos\theta) \tag{25}$$

and $\hat{c} = \kappa R/D$. This boundary condition for the surface interacting solute does not contain c_a. Species a is thus irrelevant for the particle swimming. We hence disregard c_a in this section. The concentration field c_b is determined by the differential Eq. (20) with Eq. (24). In spite of its linearity, there seems to be no analytical solution of this equation available for arbitrary $\tilde{\Psi}$. This is even so in complete absence of convection when $\mathrm{Pe}/\delta = 0$.

A. Analytical approximations

For short ranged potentials, $\lambda \ll 1$, one can resort to a technique of matched asymptotic expansions to calculate the concentration field[42]. We find for the swimming speed to lowest order in λ, (see Appendix B),

$$\begin{aligned} U_0 = \frac{\tilde{U}_0}{\hat{U}} =& \lambda^2 \frac{\kappa\, kT}{\hat{U} \eta\, D} \frac{R^2}{3} \int_0^\infty y \left(e^{-\Psi(y)} - 1\right) \mathrm{d}y = \\ & \frac{1}{3} \frac{\kappa\, kT\, L^2}{\hat{U}\, D \eta} K_1 = \frac{K_1}{3}, \end{aligned} \tag{26}$$

where $y \equiv (r-1)/\lambda$ is a dimensionless inner variable which is $O(1)$ near the surface, where Ψ changes strongly. The unnormalized moments of the equilibrium excess surface concentration are defined as

$$K_\mathrm{n} \equiv \int_0^\infty y^\mathrm{n} \left(e^{-\Psi(y)} - 1\right) \mathrm{d}y. \tag{27}$$

As in the classic electrophoretic Smoluchowski limit[43], the dimensional speed $\tilde{U}_0$ is found to be proportional to the square of the interaction lengthscale ($\sim L^2\, K_1$). We calculate the first speed correction up to $O(\lambda)$ for active diffusiophoresis by employing methods outlined by Anderson, Lowell and Prieve[42]. The corresponding first order Padé approximant of the swimming speed reads

$$\tilde{U} \approx \tilde{U}_0 / \left[1 + \lambda \left(K_0 + \frac{7\, K_2}{2\, K_1} + \frac{\mathrm{Pe}}{\delta} \frac{M}{2} + \frac{N}{K_1}\right)\right], \tag{28}$$

where the following definitions are employed

$$M \equiv \int_0^\infty \int_0^y y' \left(e^{-\Psi(y')} - 1\right) \mathrm{d}y' \left(e^{-\Psi(y)} - 1\right) \mathrm{d}y, \tag{29}$$

$$N \equiv -2 \int_0^\infty \int_0^y y' \left(e^{-\Psi(y')} - 1\right) \mathrm{d}y' \left(e^{\Psi(y)} - 1\right) \mathrm{d}y + \int_0^\infty y^2 \left(e^{-\Psi(y)} - 1\right) \left(e^{\Psi(y)} - 1\right) \mathrm{d}y. \tag{30}$$

Note that the chemical reaction must occur at a finite distance from the physical hard-core boundary of the swimmer. Therefore, the potential $\Psi(r = 1)$ cannot diverge in active diffusiophoresis and all the constants defined above remain finite.

B. Numerical results

In order to go beyond the $\lambda \ll 1$ limit, we solve Eqns. (20-22,24) numerically for the boundary conditions given in Eqns. (23,25). Results are displayed in Figs. 2, 3 and 4 where the swimming speed is plotted as $\lambda^2 U = L^2\tilde{U}/(R^2\hat{U})$ in order to demonstrate the physical dependence of the speed on the interaction length L. As it is the case for other phoretic effects[43,44], convection causes a non-monotoneous relation between particle speed and λ (Fig. 2). An increasing magnitude of the surface potential $\Psi(1)$ reduces the range of validity of the lowest order approximation U_0 to smaller values of λ (Fig. 3). The Padé approximant of U, Eq. (28), then describes the case of strong surface interactions much more satisfyingly[45]. Therefore, the Padé approximant presents a significant improvement over the lowest order estimate U_0, in spite of being useful only for $\lambda < 1$.

Fig. 4 shows the swimming speed for a truncated van der Waals-like interaction where the potential decays $\sim 1/r^6$ only far away of the swimmer. The result demonstrates that multiple lengthscales of the interaction potential may modify the simple scaling of $\tilde{U}_0 \sim L^2$. Furthermore, the similarity of the results for $\mathrm{Pe}/\delta = 0$ and $\mathrm{Pe}/\delta = 5$ qualifies the simple notion that convection of solutes reduces the speed of the particle. Since, for Fig. 4, we have $\Psi(r) \ll 1$ when $\lambda > 1$, the influence of the Peclét number is suppressed almost completely. This dependence of the effect of convection on the strength of the surface interaction also appears through the constant M in the Padé approximant given in Eqns. (28,29).

C. Comparison with passive diffusiophoresis

It is of interest to compare the swimming speed given in Eqns. (26,28) with the analogous formulae for passive diffusiophoresis in an externally imposed concentration

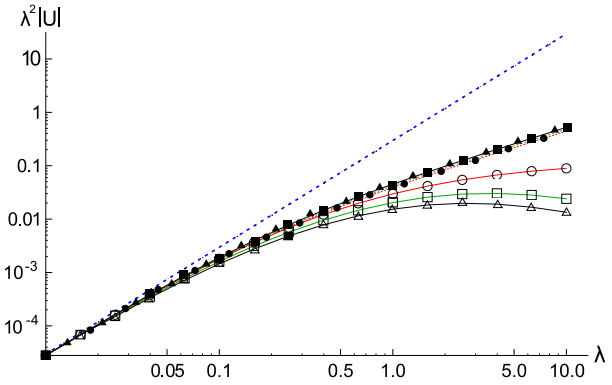

FIG. 2. Swimming speed vs. interaction lengthscale λ for an exponential repulsion: $\Psi(r) = \exp[-(r-1)/\lambda]$. (Dashed line) Swimming speed in lowest order approximation $\lambda^2|U_0|$ for $\lambda \ll 1$ from Eq. (26). (○) Numerical solution for $\mathrm{Pe}/\delta = 0$. (●) Padé approximant, Eq. (28), for $\mathrm{Pe}/\delta = 0$. (□) Numerical solution for $\mathrm{Pe}/\delta = 5$. (■) Padé approximant for $\mathrm{Pe}/\delta = 5$. (△) Numerical solution for $\mathrm{Pe}/\delta = 10$. (▲) Padé approximant for $\mathrm{Pe}/\delta = 10$.

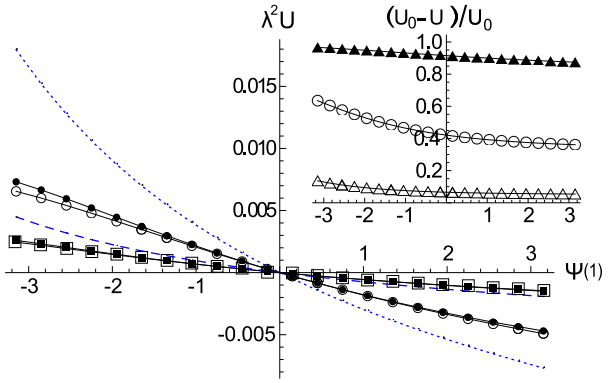

FIG. 3. Swimming speed vs. interaction potential magnitude $\Psi(1)$ for $\Psi(r) = \Psi(1)\exp[-(r-1)/\lambda]$ with $\mathrm{Pe}/\delta = 0$. (□) Numerical solution for $\lambda = 0.05$. (■) Padé approximant, Eq. (28), for $\lambda = 0.05$. (Dashed line) $\lambda^2|U_0|$ from Eq. (26) for $\lambda = 0.05$. (○) Numerical solution for $\lambda = 0.1$. (●) Padé approximant for $\lambda = 0.1$. (Dotted line) $\lambda^2|U_0|$ for $\lambda = 0.1$. Inset: Relative deviation of the lowest order approximation $(U_0 - U)/U_0$ vs. $\Psi(1)$ with $\mathrm{Pe}/\delta = 0$. (▲) $\lambda = 1$. (○) $\lambda = 0.1$. (△) $\lambda = 0.01$.

gradient[42]. Here the boundary conditions for the concentration of the solute of type b read

$$\begin{aligned} \hat{\mathbf{e}}_r \tilde{\mathbf{j}}_b(1,\theta) &= 0, \\ \nabla\tilde{c}|_\infty &= \text{const.} \times \hat{\mathbf{e}}_z. \end{aligned} \tag{31}$$

The lowest order result for swimming speed in passive diffusiophoresis $\tilde{U}^p$ is

$$\tilde{U}_0^p = |\nabla\tilde{c}|_\infty \frac{kTL^2}{\eta} K_1. \tag{32}$$

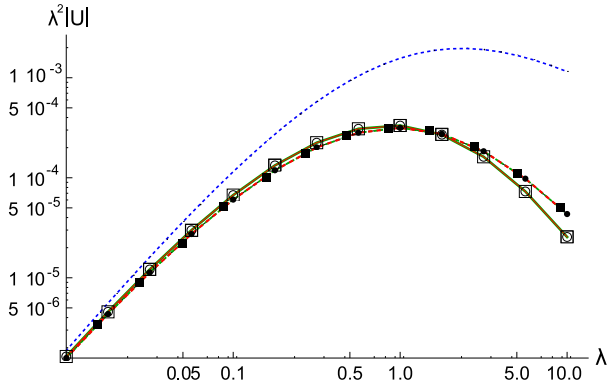

FIG. 4. Swimming speed vs. λ for a van der Waals -like attraction: $\Psi(r) = -A\lambda^3/(r-1+\lambda)^3/(r-1+\lambda+2)^3$ with $A = 1$. λ is here interpreted as solute radius divided by the swimmer radius and the potential is truncated at a distance λ away from the surface. (Dashed line) $\lambda^2|U_0|$ from Eq. (26). (○) Numerical solution for $\mathrm{Pe}/\delta = 0$. (●) Padé approximant, Eq. (28), for $\mathrm{Pe}/\delta = 0$. (□) Numerical solution for $\mathrm{Pe}/\delta = 5$. (■) Padé approximant for $\mathrm{Pe}/\delta = 5$.

The formulae (26) and (32) for active and passive swimming are, apart from a replacement of $\kappa/3D$ by $|\nabla\tilde{c}|_\infty$, the same. These different prefactors result from the dipole moments of the concentration fields around the swimmer. The concentration far away from the particle is given by $\tilde{c}_b \approx R\kappa/D\left[1/r + \cos\theta/(2r^2)\right]$ in our case and $\tilde{c}_b \approx R|\nabla\tilde{c}|_\infty\left[r + 1/(2r^2)\right]\cos\theta$ for an externally imposed concentration gradient. At $r = 1$, the self generated dipole is therefore only $\sim \kappa RD/2$ while the imposed concentration dipole is $\sim 3\,R|\nabla\tilde{c}|_\infty/2$. This leads to the differing factor of $1/3$, appearing in the swimming speeds.

The general agreement of both lowest order formulae for active and passive diffusiophoresis can be rationalized by noting that both concentrations are, in close proximity to the swimmer's surface, in radial equilibrium. Accordingly, the lowest order solute flux also vanishes for active diffusiophoresis since the diffusive exchange of solute near the active swimmer is $\sim \partial c_b/\partial(\lambda y) = O(1/\lambda)$ while the emission/absorption of solute, determined by $g(\theta)$, is only of $O(1)$.

For passive diffusiophoresis[45], the analogous formula to the first order swimming speed Eq. (28) is, in our notation,

$$\tilde{U}^p \approx \tilde{U}_0^p \Big/ \left[1 + \lambda\left(K_0 + \frac{K_2}{2\,K_1} + \frac{\mathrm{Pe}}{\delta}\frac{M}{2}\right)\right]. \qquad (33)$$

The main difference between (28) and (33) is the appearance of the term $\lambda N/K_1$ for active diffusiophoresis. The constant N, defined in Eq. (30), contains an integral over $\exp(\Psi(r))$. It increases the relative importance of the λ^1 correction for strong repulsive surface interactions. For monotonic potentials, N is a positive quantity. Therefore, the correction for active swimmers increases the swimming speed for purely repulsive interactions where we have $K_1 < 0$. Convective corrections $\sim \mathrm{Pe}/\delta$ are, both for active and passive swimming, relevant if the equilibrium concentration scale $\tilde{c}_b^{\mathrm{eq}}$ is much larger than the concentration disturbance $\hat{c}$. It is an interesting side note to the convective correction that the constant M is related to the hydrodynamic dissipation in the boundary layer[35] $\tilde{W}_{\mathrm{hyd}} \approx L^3\,M\,4\pi\,(kT\,\hat{c})^2\,/\,(3\eta)$.

V. REACTION INDUCED CONCENTRATION DISTORTION

In general, the kinetics of the chemical transformations at the swimmer's surface depend on the local concentrations and correlation functions of educts and products. An inhomogeneous reactivity profile on the swimmer, realized, e.g., through partial coating with a catalyst, couples to the angular solute distributions. Therefore, the resulting solute flux at the swimmer will usually not have the same angular dependence as the reactivity profile. We term this effect "reaction induced concentration distortion" and it bears a certain analogy to polarization phenomena, inasmuch as it has a possibly nonlinear effect on the swimming speed.

A. Boundary conditions for the concentration field

For the considered case of dilute solutions one might anticipate that the fraction of unoccupied catalytic sites on the swimmer is always very small. Then the overall reaction rates depend linearly on the concentrations of the reactants. Concentration fields resulting from nonlinear reactions[46] are beyond the scope of this article. We therefore assume, for simplicity, a reversible, first order reaction of the form $a \leftrightarrow b$. For the remainder of this article we will employ as boundary conditions for the concentration fields at $r = 1$

$$\hat{\mathbf{e}}_r\tilde{\mathbf{j}}_b(1,\theta) = (1+\cos\theta)\left[\tilde{k}_{\mathrm{ab}}\tilde{c}_a(1,\theta) - \tilde{k}_{\mathrm{ba}}\tilde{c}_b(1,\theta)\right], \qquad (34)$$

$$\hat{\mathbf{e}}_r\tilde{\mathbf{j}}_a(1,\theta) = -\hat{\mathbf{e}}_r\tilde{\mathbf{j}}_b(1,\theta), \qquad (35)$$

where $\tilde{k}_{\mathrm{ab}}$ and $\tilde{k}_{\mathrm{ba}}$ are rate constants which we nondimensionalize with D/R. The concentration dependence of the flux at the swimmer surface is also termed a radiation boundary condition. Similar mathematical problems have occurred in the calculation of mean first passage times for the combined encounter and reaction of asymmetric molecules[47,48].

In equilibrium, where the fluxes vanish, the radially symmetric distributions of solutes obey $\tilde{c}_a^{\mathrm{eq}}(r) = \tilde{c}_a^{\mathrm{eq}}(\infty)$, $\tilde{c}_b^{\mathrm{eq}}(r) = \tilde{c}_b^{\mathrm{eq}}(\infty)e^{-\Psi(r)}$ and

$$\frac{\tilde{c}_a^{\mathrm{eq}}(\infty)}{\tilde{c}_b^{\mathrm{eq}}(\infty)} = \frac{\tilde{k}_{\mathrm{ba}}e^{-\Psi(1)}}{\tilde{k}_{\mathrm{ab}}}. \qquad (36)$$

A finite reaction rate at the swimmer's surface is ultimately driven by chemical potential differences far away, at the boundary of the system. Expressions

for the chemical potentials are given in Appendix A. Within the linear response regime we expect that $\left(\tilde{c}_{\{a,b\}}(\infty)/\tilde{c}^{\rm eq}_{\{a,b\}}(\infty)-1\right)\ll 1$. Therefore, the chemical potential difference at $\tilde{r}\to\infty$ becomes

$$\Delta\mu_\infty \equiv \frac{\tilde{\mu}_a(\infty)-\tilde{\mu}_b(\infty)}{kT} \approx \frac{\tilde{c}_a\left(\infty\right)}{\tilde{c}^{\rm eq}_a(\infty)}-\frac{\tilde{c}_b\left(\infty\right)}{\tilde{c}^{\rm eq}_b(\infty)} = \frac{1}{\tilde{k}_{\rm ab}\tilde{c}^{\rm eq}_a}\left[\tilde{k}_{\rm ab}\,\tilde{c}_a(\infty)-\tilde{k}_{\rm ba}e^{-\Psi(1)}\,\tilde{c}_b(\infty)\right]. \tag{37}$$

The concentration scale Eq. (13) can now be defined as

$$\hat{c}=\frac{R}{D}\,\tilde{k}_{\rm ab}\,\tilde{c}^{\rm eq}_a(\infty)\,\Delta\mu_\infty = k_{\rm ba}\,\tilde{c}^{\rm eq}_b(\infty)e^{-\Psi(1)}\,\Delta\mu_\infty \tag{38}$$

and from Eq. (4) with Eq. (34) we have $g(\theta)=\hat{\mathbf{e}}_r\tilde{\mathbf{j}}_b(1,\theta)\times R/(D\,\hat{c})$. The parameter δ and the velocity scale $\hat{U}$ are accordingly given by

$$\delta=\frac{\hat{c}}{\tilde{c}^{\rm eq}_b(\infty)}=\Delta\mu_\infty e^{-\Psi(1)}\,k_{\rm ba}, \tag{39}$$

$$\hat{U}=\frac{kTL^2}{\eta}\frac{k_{\rm ab}\tilde{c}^{\rm eq}_a\Delta\mu_\infty}{R}. \tag{40}$$

In order to calculate the concentration perturbations $c_{\{a,b\}}$ around the swimmer we proceed by expanding them in Legendre polynomials $P_n(\cos\theta)$ as

$$\begin{aligned} c_a =& c_a\left(\infty\right)+\sum_{n=0}^{\infty}c^n_a(r)P_n\left(\cos\theta\right),\\ c_b =& c_b\left(\infty\right)e^{-\Psi(r)}+\sum_{n=0}^{\infty}c^n_b(r)P_n\left(\cos\theta\right), \end{aligned} \tag{41}$$

which includes the boundary conditions at $r\to\infty$. The boundary conditions at the surface of the swimmer, Eqns. (34,35), couple different coefficients of the expansion Eq. (41) and one has

$$\frac{-2}{2n+1}\left[\partial_r c^n_b+c^n_b\partial_r\Psi\right]|_{r=1}=\int_0^\pi P_n\left(\cos\theta\right)g(\theta)\sin\theta{\rm d}\theta, \tag{42}$$

$$-\left[\partial_r c^n_b+c^n_b\partial_r\Psi\right]|_{r=1}=\left[\partial_r c^n_a\right]|_{r=1}. \tag{43}$$

B. Analytical approximations

We consider a swimmer with short interaction length $\lambda\ll 1$. Employing the methods presented in Appendix B we calculate the concentration fields to leading order in λ. Far away of the swimmer, where $\Psi(r)\to 0$, Eqns. (20,24) can be replaced by Laplace's equations and we have $c^n_{\{a,b\}}(r)=A^n_{\{a,b\}}/r^{n+1}$ in Eq. (41). For c_a, this expansion is valid throughout the whole system. For the b-type solute we have to leading order near the surface of the swimmer $c^n_b(y)\approx a^n_b e^{-\Psi(y)}$. Matching these solutions and employing the boundary condition Eq. (43) leads to $a^n_b=A^n_b=-A^n_a$. Finally, Eq. (42) yields a recursion equation for the constants A^n_b

$$\begin{aligned} &\left[2\delta_{n,0}+\frac{2}{3}\delta_{n,1}\right]=\\ &\frac{2\left(n+1+k_+\right)}{2n+1}A^n_b+\frac{2n\,k_+}{(2n+1)\,(2n-1)}A^{n-1}_b+\\ &\frac{2(n+1)k_+}{(2n+1)\,(2n+3)}A^{n+1}_b. \end{aligned} \tag{44}$$

Here we defined

$$k_+\equiv k_{\rm ab}+k_{\rm ba}e^{-\Psi(1)}=k_{\rm ab}\left(1+\frac{\tilde{c}^{\rm eq}_a\left(\infty\right)}{\tilde{c}^{\rm eq}_b\left(\infty\right)}\right). \tag{45}$$

Eq.(44) can be written in matrix form as $B_j=M_{jn}\,A^n_b$. The off-diagonal elements of $\{M_{jn}\}$ decay like $\sim 1/n$ and we can invert a finite matrix $\{M_{jn}\}$ to determine a numerical approximation of the $\{A^n_b\}$. In the following, plots of analytical results involving A^n_b, are created by employing Eq. (44) and $n_{\rm max}=70$. Since $\Psi(r)$ is radially symmetric, the swimming speed depends only on the dipole moment of the concentration field. Accordingly, an expansion of Eq. (10) for small λ yields for the lowest order the free swimming speed

$$\tilde{U}_0=\hat{U}\frac{K_1}{3}\,2A^1_b. \tag{46}$$

For small bare rates, and therefore small k_+, one can expand the inner concentration field of the b-type solute

$$\begin{aligned} c_b =& c_b(\infty)e^{-\Psi(r)}+e^{-\Psi(r)}\times\\ &\left[A^0_b+A^1_b\cos\theta+A^2_bP_2(\cos\theta)+A^3_bP_3(\cos\theta)+O(k^3_+)\right] \end{aligned} \tag{47}$$

with following approximations for the constants

$$A^0_b\approx\frac{42+2k_+}{42+51k_+},\qquad A^1_b\approx\frac{135-26k_+}{270+353k_+}, \tag{48}$$

$$A^2_b\approx-\frac{2k_+}{18+33k_+},\qquad A^3_b\approx\frac{k^2_+}{60}. \tag{49}$$

The magnitude of the dipole moment is determined by $A^1_b\approx(1/2-3k_+/4)$. Reaction induced concentration distortion, emerging here through the corrections in orders of k_+, reduces the dipole moment and thus slows the particle swimming down.

C. Numerical results

To complement the analytical approximations, we calculate the swimming speed numerically. Eqns. (34,35) with fixed concentrations far away of the swimmer are employed for numerical solution of Eqns. (20-24). The boundary conditions result in an infinite system of equations where the solute concentrations far away of the

swimmer $c_{\{a,b\}}(\infty)$ determine the reaction speed. The system can be truncated above a certain order $n_{\max}$ of the Legendre polynomials. In choosing here $n_{\max} = 4$ we made sure that the error in the calculated concentrations is negligible. Fig. 5 contains an exemplary plot of how the reaction induced concentration distortion influences the swimming speed U. The chosen velocity scale $\hat{U}$ (Eq. 40) contains the linear dependence on $c_{\{a,b\}}(\infty)$. With

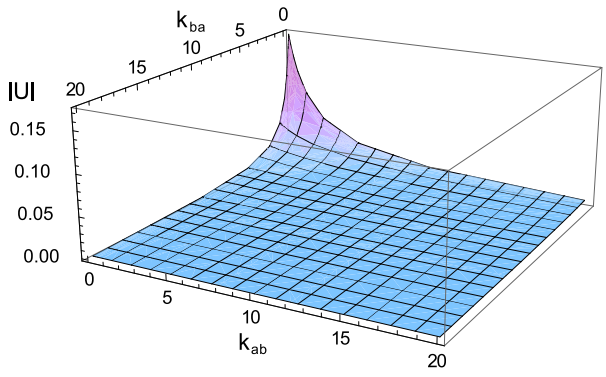

FIG. 5. Particle speed U as a function of $k_{\rm ab}$ and $k_{\rm ba}$ for $\Psi(r) = \exp\left[-(r-1)/\lambda\right]$, $\mathrm{Pe}/\delta = 1$ and $\lambda = 0.1$.

the employed first order reactions, the concentration distortion depends nonlinearly on the bare rates $k_{\rm ab}$ and $k_{\rm ba}$ but linearly on the concentration scales $c_{\{\rm a,b\}}(\infty)$. Thus, in an experiment in the linear regime, with fixed $k_{\rm ab}$ and $k_{\rm ba}$, the reaction induced concentration distortion might be accounted for by a constant prefactor, modifying the swimming speed.

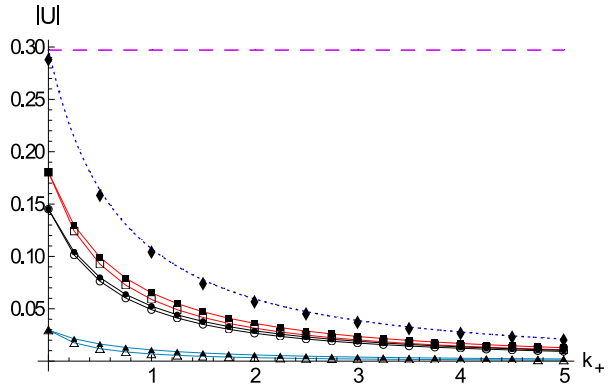

FIG. 6. Rate constant dependence of the swimming speed U for $\Psi(r) = \exp\left[-(r-1)/\lambda\right]$. See Eq. (45) for the definition of k_+. (Dashed line) Reaction induced concentration distortion neglected as explained in the text, leading to $U = K_1/3$ with $K_1 \simeq -0.89$. (Dotted line) Approximation U_0 (Eq. (46)) for $\lambda \ll 1$ which takes the concentration distortion into account. Full symbols are numerical results for $k_{\rm ba} = 0$ and open symbols are results for $k_{\rm ab} = 0$. (♦) $\lambda = 0.005$, $\mathrm{Pe}/\delta = 0$. (■,□) $\lambda = 0.1$, $\mathrm{Pe}/\delta = 0$. (●,○) $\lambda = 0.1$, $\mathrm{Pe}/\delta = 10$. (▲,△) $\lambda = 1$, $\mathrm{Pe}/\delta = 0$.

In Fig. 6 we plot numerical results for the swimming speed as a function of k_+, defined in Eq. (45). Neglecting the reaction induced concentration distortion, the naive boundary condition for the concentration would be $\hat{\mathbf{e}}_r \mathbf{j}_b|_{r=1} = (1 + \cos\theta)$. The resulting swimming speed is independent of k_+. It agrees with the analytical approximation in Eq. (46) in the limit $k_+ \to 0$. However, Fig. 6 shows that neglecting reaction induced concentration distortion in this way leads to significant errors in the speed estimate for finite reaction rate constants. The analytical approximation, Eq. (46), is found to be useful for $\lambda \lesssim 0.01$.

Fig. 7 shows the dependence of swimming speed on the strength of the interaction potential $\Psi(1)$. The symmetry between the effects of changing $k_{\rm ab}\exp\left(-\Psi(1)\right)$ and $k_{\rm ba}$, apparent in the parameter k_+ in U_0 when $\lambda \ll 1$, is lost for finite λ. Increasing the strength of the interaction potential $\Psi(1)$ makes this asymmetry more pronounced.

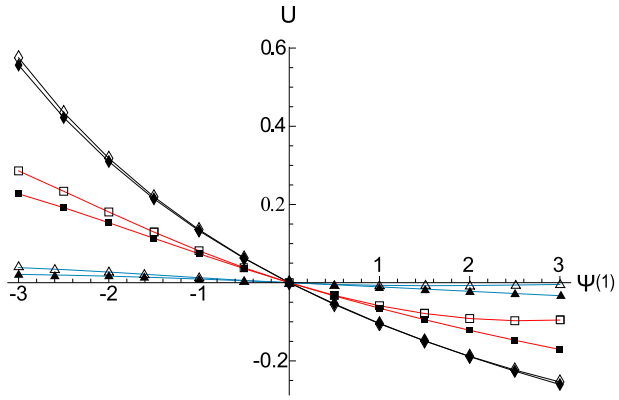

FIG. 7. Swimming speed as a function of the potential strength $\Psi(1)$. Numerical results are computed with $\Psi(r) = \Psi(1)\exp\left[-(r-1)/\lambda\right]$ and $\mathrm{Pe}/\delta = 0$. Full symbols indicate ($k_{\rm ab} = 1$, $k_{\rm ba}\exp\left(\Psi(1)\right) = 0$). Open symbols indicate ($k_{\rm ab} = 0$, $k_{\rm ba}\exp\left(\Psi(1)\right) = 1$). (♦,◊) $\lambda = 0.005$. (■,□) $\lambda = 0.1$. (▲,△) $\lambda = 1$.

VI. ENERGETICS

A. Energy balance

We consider an isothermal situation (T = const.) where the system, i.e., the swimmer and the multicomponent fluid is in a steady state. The steady state implies, that the molecules which are modified by a chemical reaction need to be replenished from outside the system. To do this in a real experiment, one would need to connect some sort of external apparatus to the system. We idealize the apparatus by a reversible process consuming the power $\tilde{P}_{\rm in}$. The total of external apparatus and system does not exchange matter with the external world. Therefore $\tilde{P}_{\rm in}$ is balanced by the overall heat

outflow from the system and apparatus. On employing classical, linear nonequilibrium thermodynamics we find the power input (see Appendix C)

$$\tilde{P}_{\rm in} = kT\,\hat{c}DR \int \left(\Theta_{\rm hyd} + \Theta_{\rm diff} + \Theta_{\rm react}\right)\,{\rm d}V. \qquad (50)$$

The power is consumed by the following three entropy production rates per volume $\Theta_{(...)}$

$$\Theta_{\rm hyd} \equiv -{\rm Pe}\,\mathbf{v}\left(c_b + \frac{e^{-\Psi}}{\delta}\right)\nabla\Psi, \qquad (51)$$

$$\Theta_{\rm diff} \equiv -\mathbf{j}_b\nabla\Psi - \sum_i \mathbf{j}_i\nabla\mu_i, \qquad (52)$$

$$\Theta_{\rm react} \equiv \delta\,(r-1)\,g(\theta)\,(\mu_a - \Psi - \mu_b)\,. \qquad (53)$$

The integral over $\Theta_{\rm hyd}$ is the overall hydrodynamic work because no external force is applied to the swimmer and because $\nabla\cdot\mathbf{v} = 0$. Its proportionality to Pe emphasizes an interpretation as convection of b-type solute within the potential Ψ. Furthermore, convection of solutes also modifies the reaction rate through the mass action law underlying the definition of $g(\theta)$. Hence, the common neglect of convection in dynamical problems[30] would make an overall energy balance within the chosen framework impossible. In the linear response regime the power consumption up to $O(\delta^2)$ can be rewritten for the employed model as (see Appendix C)

$$\tilde{P}_{\rm in} = kTD\hat{c}R \int \mathbf{J}_b\Delta\mu_\infty\hat{\mathbf{e}}_r{\rm d}A_{r=\infty}. \qquad (54)$$

Note that $\Delta\mu_\infty$ is the chemical potential difference at the outer boundary of the system, not the local chemical potential difference at the the reaction site. Eq. (54) is nothing but the free energy exchange between the system and the apparatus. Due to the similarity of masses and sizes of the fluid constituents, it does not make a difference whether we consider a fixed pressure at the outer boundaries of the system or a fixed system size.

B. Efficiency of swimming

Our freely moving swimmer does not have an external power output which could be employed to calculate its efficiency. Still, one might ask how efficient this swimmer can transport itself. A natural way to do this, is to compare the energy dissipation of active swimming with the energy dissipation taking place when dragging the same particle. We accordingly define a swimming efficiency as

$$\begin{aligned}\epsilon \equiv & \frac{6\pi\eta R\,\tilde{U}^2}{\tilde{P}_{\rm in}} = {\rm Pe}\,\lambda^2\frac{6\pi\,U^2}{\int \mathbf{J}_b\Delta\mu_\infty\,\hat{\mathbf{e}}_r{\rm d}A_{r=\infty}} = \\ & \frac{\rm Pe}{\delta}\,k_{\rm ba}e^{-\Psi(1)}\lambda^2\frac{6\pi\,U^2}{\int \mathbf{J}_b\hat{\mathbf{e}}_r{\rm d}A_{r=\infty}},\end{aligned} \qquad (55)$$

where we have used Eq. (39) in the second line. The numerator of Eq. (55) is the hydrodynamic dissipation of a passively dragged sphere and the denominator is the power consumption of our external apparatus, providing the energy for active swimming. This definition is a natural extension to Lighthill's formula for hydrodynamic efficiency[49]. The power consumption $\tilde{P}_{\rm in}$ is bounded from below by the hydrodynamic dissipation $2\eta\int\tilde{\mathbf{E}}:\nabla\tilde{\mathbf{v}}\,{\rm d}\tilde{V}$. This intuitive result follows formally in Eq. (50) from the linear force-flux relationships. Since[35] $6\pi\eta R\tilde{U}^2 \le 2\eta\int\tilde{\mathbf{E}}:\nabla\tilde{\mathbf{v}}\,{\rm d}\tilde{V}$, we always have $\epsilon \le 1$ as long as no approximation is used to evaluate Eq. (55).

C. Analytical approximation for the efficiency of swimming

In the limit $\lambda \ll 1$ one can employ the lowest order speed $\tilde{U}_0$, Eq. (46), for the calculation of the efficiency from Eq. (55). The result, including the effect of reaction induced concentration distortion, is

$$\begin{aligned}\epsilon \approx & \lambda^2\,{\rm Pe}\,\frac{6\pi}{4\pi\,A_b^0\Delta\mu_\infty}\left(\frac{2}{3}A_b^1K_1\right)^2 = \\ & \frac{D_S}{D}\,\frac{L^4\,\hat{c}}{R}\,\frac{kT}{\Delta\tilde{\mu}_\infty}\,\frac{4\pi\,\left(A_b^1K_1\right)^2}{A_b^0},\end{aligned} \qquad (56)$$

where we have employed the translational diffusion constant of the swimmer $D_{\rm S} = kT/6\pi\eta R$. The first three dimensionless groups in the second line of Eq. (56) determine the magnitude of the efficiency. As discussed in our previous work[35], (nano-) swimmers with interaction lengths comparable to their size can have a higher efficiency than swimmers with $L \ll R$. This is is evident from the factors $D_{\rm S}/D$ and $\hat{c}\,L^4/R = \hat{c}L^3\times\lambda$ in Eq. (56). We evaluate Eq. (56) by employing the parameters A_b^0, A_b^1 calculated from Eq. (44) with $n_{\rm max} = 70$. The results agrees with numerical solutions for Eq. (55) (see below) when $\lambda \lesssim 0.01$. However, ignoring convection in the denominator of Eq. (55) due to the small λ limit implies neglecting hydrodynamic dissipation. Therefore, the asymptotic efficiency in Eq. (56) is not strictly bounded by unity.

D. Numerical results for the efficiency of swimming

For a numerical evaluation of Eq. (55) we truncate the expansion in Legendre polynomials at $n_{\rm max} = 4$ as in Sec. V. Due to the linear response nature of our theory, numerator and denominator of Eq. (55) are both quadratic in $\Delta\mu_\infty$. Therefore, the equilibrium perturbation driving the motion of the swimmer does not appear in the efficiency. However, the results support the notion that the swimming efficiency increases away from the quasi-equilibrium limit.

As seen in Figs. 8 and 9, the swimming efficiency is proportional to $\lambda^2\,{\rm Pe}\,/\delta \sim L^4$ for $\lambda \ll 1$. This scaling is also evident from the prefactor in Eq. (55). With a fixed Peclét number, ${\rm Pe}\,/\delta > 0$, the swimming efficiency decreases for $\lambda \gtrsim 1$ (Fig. 8). Comparison with Fig. 2 shows that the reduction in efficiency is due to the

reduction of swimming speed in this regime. When, for $\lambda \gtrsim 1$, the swimming speed does not increase $\sim \lambda^2$, fixing the Peclét number in Eq. (55) introduces a scaling of ϵ with a negative power of λ. As an alternative, one could remove the dependence of Pe on the interaction lengthscale L by setting $\mathrm{Pe}/(\delta\lambda^2) = \text{const}$ for Fig. 8. This way of plotting the data would render the decrease of ϵ for $\lambda \gtrsim 1$ less pronounced.

According to Eqns. (19,39,40), fixing Pe/δ and λ implicitly sets an absolute equilibrium concentration scale. Therefore, Fig. 9 also suggests that the efficiency of diffusiophoretic swimming increases with the absolute concentration scale for $\lambda \lesssim 1$. Only the asymptotic analytical result for $\lambda = 0.01$ has been plotted in Fig. 9 because the curve for $\lambda = 0.1$ already showed significant deviations from the numerical data.

Fig. 10 shows the dependence of the swimming efficiency on the strength of the interaction potential $\Psi(1)$. $\Psi(1)$ influences both, the reaction rate and the swimming speed and therefore it has a nonlinear effect on ϵ. Reaction induced concentration distortion plays an important role for the shape of the curve, in particular for $\Psi(1) < 0$ when k_+ can become much larger than unity. For $\Psi(1) \to 0$ the swimming efficiency vanishes.

Figure 11 shows the swimming efficiency for fixed equilibrium constant $\tilde{c}_a^{\mathrm{eq}}(\infty)/\tilde{c}_b^{\mathrm{eq}}(\infty)$ and varying reaction rate k_{ba}. For simplicity, we consider here only $\lambda = 0.01 \ll 1$. Due to the truncation of the full numerical solution at Legendre polynomials of the order $n_{\max} = 4$ the error in the numerical data becomes large beyond the plotted range. The reaction induced concentration distortion again explains major features of the plotted curves. For $k_{\mathrm{ba}} \exp(-\Psi(1)) \ll 1$ and $k_{\mathrm{ba}} \exp(-\Psi(1)) \lesssim \tilde{c}_a^{\mathrm{eq}}(\infty)/\tilde{c}_b^{\mathrm{eq}}(\infty)$ the reaction induced concentration distortion is negligible. Then ϵ rises linearly with k_{ba} and the curves fall onto each other. For larger equilibrium constants with $\tilde{c}_a^{\mathrm{eq}}(\infty)/\tilde{c}_b^{\mathrm{eq}}(\infty) \gg 10$ the location of the maximum of swimming efficiency becomes becomes independent of the equilibrium constant. On employing Eq. (56) we here find the maximum of ϵ at $k_{\mathrm{ba}} \simeq 1.13 \exp \Psi(1)$.

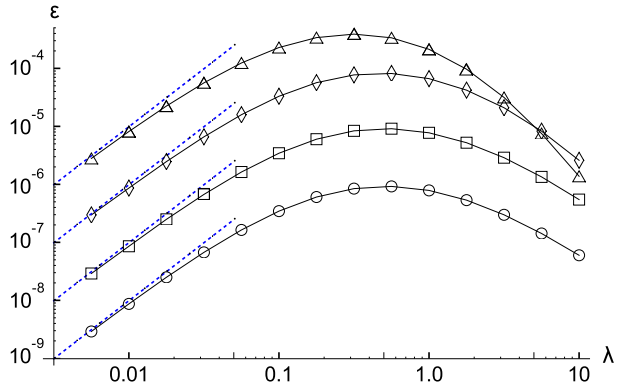

FIG. 8. The swimming efficiency ϵ as a function of λ with constant Pe/δ for $\Psi(y) = \exp[-(r-1)/\lambda]$ and $k_{\mathrm{ab}} = k_{\mathrm{ba}} = 1$. (Dashed lines) Asymptotic results calculated from Eq. (56). (△) $\mathrm{Pe}/\delta = 10$. (◇) $\mathrm{Pe}/\delta = 1$. (□) $\mathrm{Pe}/\delta = 0.1$. (○) $\mathrm{Pe}/\delta = 0.01$.

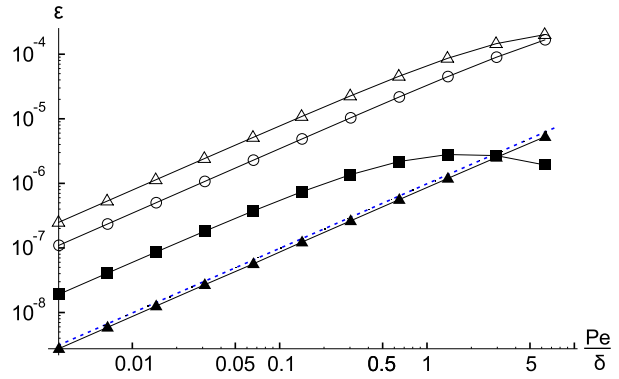

FIG. 9. The swimming efficiency ϵ as a function of Pe/δ with constant λ for $\Psi(y) = \exp[-(r-1)/\lambda]$, $k_{\mathrm{ab}} = k_{\mathrm{ba}} = 1$. (Dashed line) Asymptotic result for $\lambda = 0.01$ calculated from Eq. (56). (■) $\lambda = 10$. (△) $\lambda = 1$. (○) $\lambda = 0.1$. (▲) $\lambda = 0.01$.

E. Efficiency of transport

The definition of swimming efficiency in Eq. (55) is based on the comparison of energy dissipation per unit time. In certain practical applications of diffusiophoresis one might prefer other efficiency measures. It is, e.g., interesting to have a measure for the energetic cost of using active swimmers for transport between two locations. Then, it may be more appropriate to compare energy dissipation per transport distance. For concreteness, we think here of a slab geometry which the swimmers are to cross. Thereby, they move from one slab at $\tilde{x} = 0$ to the other slab at $\tilde{x} = \tilde{X} > 0$. Since the swimmers are freely suspended, they will not swim straightly but Brownian, translational and rotational, diffusion comes into play. The translational diffusion has a constant $D_{\mathrm{S}} = kT/(6\pi\eta R)$ and the rotational diffusion happens on a timescale $\tau_{\mathrm{rot}} = 8\pi\eta R^3/kT$. For long times $\tilde{t} \gg \tau_{\mathrm{rot}}$, one can employ an effective translational diffusion constant[16,19,33,50] where the effects of random diffusion and active, translational motion are incorporated as $D_{\mathrm{eff}} = D_{\mathrm{S}} + \tilde{U}^2 \tau_{\mathrm{rot}}/6$. This approach neglects possible modifications of D_{S} and τ_{rot} due to the active processes. In our setup we expect the transport distance $\tilde{X}$ to be much larger than a characteristic length of the random walk $\tilde{X} \gg D_{\mathrm{eff}}/|\tilde{U}|$. Employing reflecting boundary conditions at $\tilde{x} = 0$, the mean first passage time $\tilde{t}_{\mathrm{mf}}$ to reach $\tilde{x} = \tilde{X}$ is simply given by $\tilde{t}_{\mathrm{mf}} = \tilde{X}^2/(2D_{\mathrm{eff}})$. The energy consumed by the swimmer during the time $\tilde{t}_{\mathrm{mf}}$ can be estimated by $\tilde{P}_{\mathrm{in}} \tilde{t}_{\mathrm{mf}}$. For an energetic comparison, one might consider dragging a passive particle directly across $\tilde{X}$. The corresponding dissipated work would be $6\pi\eta R|\tilde{U}|\,\tilde{X}$. Hence, we define a new efficiency of trans-

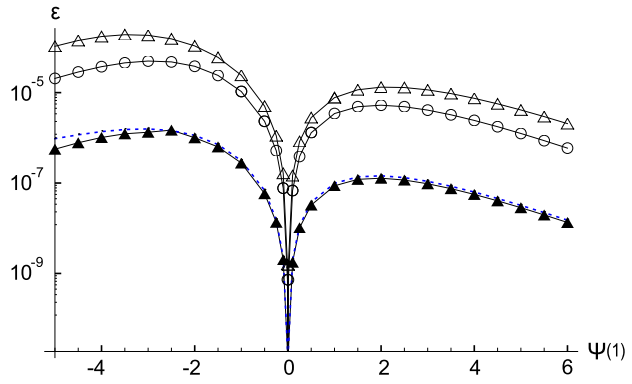

FIG. 10. Swimming efficiency ϵ vs. the strength of the interaction potential $\Psi(1)$, where $\Psi(y) = \Psi(1)\exp[-(r-1)/\lambda]$, $k_{\rm ab} = k_{\rm ba} = 1$ and $\mathrm{Pe}/\delta = 0.1$. (Dashed line) Asymptotic result for $\lambda = 0.01$ calculated from Eq. (56). (△) $\lambda = 1$. (○) $\lambda = 0.1$. (▲) $\lambda = 0.01$.

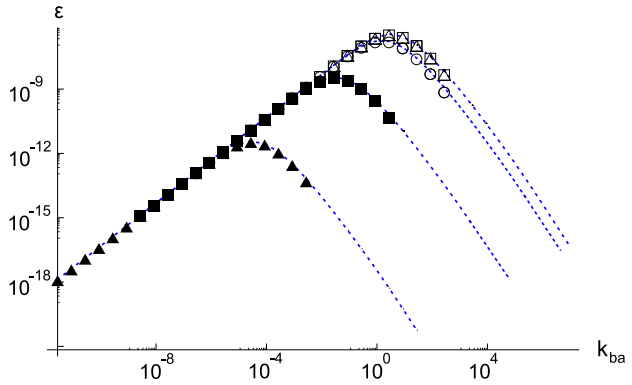

FIG. 11. Dependence of the swimming efficiency ϵ on the reaction rate constant $k_{\rm ba}$ with fixed equilibrium constant $K_{\rm a} \equiv \tilde{c}_a^{\rm eq}(\infty)/\tilde{c}_b^{\rm eq}(\infty)$ and $\mathrm{Pe}/\delta = 0.1$, $\lambda = 0.01$, $\Psi(y) = \exp[-(r-1)/\lambda]$. (Dashed lines) Asymptotic results calculated from Eq. (56). (▲) $K_{\rm a} = 10^{-5}$. (■) $K_{\rm a} = 10^{-2}$. (○) $K_{\rm a} = 1$. (□) $K_{\rm a} = 10^{2}$. (△) $K_{\rm a} = 10^{5}$.

port as

$$\epsilon_{\rm transp} \equiv \frac{6\pi\eta R|\tilde{U}|\,\tilde{X}}{\tilde{P}_{\rm in}\,\tilde{t}_{\rm mf}} = \epsilon\,\frac{\tilde{X}}{|\tilde{U}|\,\tilde{t}_{\rm mf}}, \qquad (57)$$

which we relate on the right hand side to the efficiency of swimming ϵ through Eq. (55). On employing the result for the mean first passage time $\tilde{t}_{\rm mf}$ given in the text above we find

$$\epsilon_{\rm transp} = \frac{\epsilon}{\tilde{X}}\,\frac{2D_{\rm eff}}{|\tilde{U}|} = \frac{\epsilon}{\tilde{X}}\left(\frac{2D_{\rm S}}{|\tilde{U}|} + \frac{|\tilde{U}|\tau_{\rm rot}}{3}\right). \qquad (58)$$

This dependence $\sim 1/\tilde{X}$ of the relative energetic cost of direct transport compared to enhanced diffusion is a quite generic result. It emphasizes the necessity to impose a directionality on the active motion if the transport distance is to be of macroscopic size.

VII. DISCUSSION AND CONCLUSION

In the present publication we take a close look at the dynamics and efficiency of diffusiophoretic swimming in the linear response regime. In Sec. IV we analyze the role of the surface interaction potential with regard to the dynamics of the swimmer. If the lengthscale of the interaction potential is not negligible compared to the swimmer radius ($\lambda \gtrsim 0.01$), the details of the interaction become important. Analytical corrections in powers of λ to the lowest order swimming speed include various moments of the solute concentration and also the effect of solute convection. These corrections occur for active diffusiophoresis in a qualitatively similar way as for passive diffusiophoresis[51]. A particular feature of active diffusiophoresis, however, is that the emission of solutes can cause an increase of speed for repulsive surface interactions. The enhanced speed reflects the effect of "producing" solutes directily inside the region from which they are repelled.

In Sec. V we employ a linear reaction scheme to model the active conversion of solutes at the swimmer's surface. Concentration dependent boundary conditions result in a strong modification of the concentration fields as compared to fixing the flux of solutes at the boundary. This reaction induced concentration distortion also occurs in the limit $\lambda \ll 1$ and has a pronounced effect on the swimming speed. In the linear response regime it causes a reduction of the swimming speed, independent of the absolute concentration levels. If the reaction rate becomes nonlinear in the concentrations, a measurable, concentration dependent, speed modification is to be expected. The whole effect may vanish only in the strongly reaction limited regime of very high substrate concentrations.

In Sec. VI we present results concerning the efficiency of diffusiophoretic swimming. The active motion considered in the present publication is energetically quite distinct from classical phoresis in external gradients[30] . For the latter systems, the absolute level of concentration changes when the particle moves in an externally applied gradient. In our case the absolute concentrations remain, on average, the same; which implies, that our system can be held in a true steady state. The studied model includes three modes of entropy production namely hydrodynamic dissipation, dissipation in the chemical reaction and entropy production through diffusion of solutes. While the former two can be recognized immediately as contributions to the power input, the latter becomes only meaningful when considering an external apparatus, which converts free energy exchange at the outer boundaries of the system into work. Identification of the power consumption with the free energy exchange at the outer boundaries of the system is a consequence of the spatial modelling of the process. It is a natural extension to the commonly employed formalism for biomolecular motors[52], where the local free energy exchange rate is taken as work input. It is pivotal for the energy balance to recognize of the importance of convec-

tion. For illustration, we think of a situation where the reaction rates would be fully independent of the fluid motion. This would mean that the net exchange of solutes with the external apparatus would be independent of the motion of the particle. Thus, according to Eq.(54), the power input would be independent of the hydrodynamic dissipation, which violates energy conservation. Within this model, the only way how the particle speed may feedback on the chemical reaction is via a convective modification of the concentrations. This link leads, together with the mass-action law, to a proper energy balance.

Relying on the robustness of the scaling of the efficiency $\epsilon \sim D_s/D \times L^4\hat{c}/R$ (Eq. (56)), one can employ experimental values for catalytic swimmers to estimate their efficiency. For swimmers with size in the $1\,\mu m$ range, we have $D_s/D \simeq 10^{-4}$. Given a concentration scale[33] of $\hat{c} \simeq 10^7\,1/\mu m^3$ and an interaction length of $L \simeq 1\,\mathrm{nm}$ we have $L^4\hat{c}/R = 10^{-5}$. Together we find $\epsilon \simeq 10^{-9}$. This number corresponds to the experimental estimate for the swimmers of Paxton et. al[3]. The agreement may, however, be incidental since these swimmers are operating mainly with a self-electrophoretic mechanism instead of the diffusiophoretic mechanism studied here. Naturally, if the concentration perturbation $\hat{c}$ is caused by a large chemical potential difference, this may also affect the efficiency as seen from Eq. (56).

In conclusion, we expect the main relevance of this work to lie in the scaling predictions and in the identification of the main trends in the numerical data. A more detailed modeling of specific phoretic mechanisms is challenging, but desirable. One interesting question is to replace the conservative potential Ψ by more realistic, angular dependent surface interactions. In reality, the solute-swimmer interactions may even transfer energy between the fluid and microscopic degrees of freedom on the swimmer's surface. Thus, they can acquire a "dissipative nature", possibly resulting in an effective modification of the viscosity around the swimmer. Also, lateral diffusion of solutes adsorbed to the surface of the swimmer could be taken into account here. Issues like hydrodynamic surface slip[53] may further complicate the situation. For a full description of the behavior of catalytically driven swimmers one must also go beyond the linear response theory. This refinement of the model will particularly effect the reaction induced concentration distortion. Finally, the predictions for the scaling of the swimming speed and efficiency offer the possibility of being experimentally tested, which could add interesting new facets to the picture of diffusiophoresis presented here.

Appendix A: Simple model for the dilute solution

In this Appendix we provide a simple, but detailed derivation of the model fluid employed in the main part of the text. We denote the molecular masses of the solutes and solvent by m_a,m_b and m_s. The molecular volumes are constants, denoted by v_a,v_b and v_s respectively. The volume variable is written as $\tilde{V}$. We define a local, position dependent free energy per unit volume $\tilde{f} \equiv \tilde{F}/\tilde{V}$ as

$$\tilde{f}(\tilde{c}_a,\tilde{c}_b,\tilde{c}_s) \equiv \phi\tilde{\Psi}_0 + \tilde{c}_b v_b\tilde{\Psi}_1 + \tilde{c}_b\epsilon_b + \tilde{c}_a\epsilon_a + \frac{\chi}{2}(\phi-1)^2 + kT\left[\tilde{c}_a\log\left(\frac{\tilde{c}_a v_a}{\phi}\right) + \tilde{c}_b\log\left(\frac{\tilde{c}_b v_b}{\phi}\right) + \tilde{c}_s\log\left(\frac{\tilde{c}_s v_s}{\phi}\right)\right], \tag{A1}$$

where $\phi \equiv \tilde{c}_a v_a + \tilde{c}_b v_b + \tilde{c}_s v_s$. Here the surface interactions between the fluid constituents and the swimmer are incorporated through the potential energies per volume $\tilde{\Psi}_0$ and $\tilde{\Psi}_1$. ϵ_a,ϵ_b are the internal energies of the solutes of type a and b respectively. The local, hydrostatic pressure is calculated as

$$\tilde{p} = -\frac{\mathrm{d}\left(\tilde{f}\tilde{V}\right)}{\mathrm{d}\tilde{V}} = -\tilde{f} + \frac{\partial\tilde{f}}{\partial\tilde{c}_a}\tilde{c}_a + \frac{\partial\tilde{f}}{\partial\tilde{c}_s}\tilde{c}_s + \frac{\partial\tilde{f}}{\partial\tilde{c}_s}\tilde{c}_s = \frac{\chi}{2}\left[\phi^2-1\right]. \tag{A2}$$

In the incompressible limit one has $\phi = (\tilde{c}_a v_a + \tilde{c}_b v_b + \tilde{c}_s v_s) \approx 1$ and the pressure can be expanded as $\tilde{p} \approx \chi\,[\phi-1]$. The generalized chemical potentials $\tilde{\mu}_i' \equiv \tilde{\mu}_i + v_i\left(\tilde{\Psi}_0 + \delta_{i,b}\tilde{\Psi}_1\right) = \partial\tilde{f}/\partial\tilde{c}_i$ become, with $\tilde{c}_{all} \equiv (\tilde{c}_a + \tilde{c}_b + \tilde{c}_s)$,

$$\tilde{\mu}_s' \approx kT\left[\log\left(\tilde{c}_s v_s\right) - \tilde{c}_{all} v_s\right] + v_s\left(\tilde{\Psi}_0 + \tilde{p}\right) + kT\left(v_s\tilde{c}_{all} - 1\right)(\phi-1), \tag{A3}$$

$$\tilde{\mu}_a' \approx kT\left[\log\left(\tilde{c}_a v_a\right) - \tilde{c}_{all} v_a\right] + \epsilon_a + v_a\left(\tilde{\Psi}_0 + \tilde{p}\right) + kT\left(v_a\tilde{c}_{all} - 1\right)(\phi-1), \tag{A4}$$

$$\tilde{\mu}_b' \approx kT\left[\log\left(\tilde{c}_b v_b\right) - \tilde{c}_{all} v_b\right] + \epsilon_b + v_b\left(\tilde{\Psi}_0 + \tilde{\Psi}_1 + \tilde{p}\right) + kT\left(v_b\tilde{c}_{all} - 1\right)(\phi-1). \tag{A5}$$

We now apply the highly simplifying assumption of symmetric solute constituents

$$v_a \simeq v_b \simeq v_s, \tag{A6}$$

$$m_a \simeq m_b \simeq m_s \tag{A7}$$

through which particle and mass fluxes become equivalent. Also, we assume that the volume fraction of solvent is much larger than that of the solute

$$\tilde{c}_a v_a + \tilde{c}_b v_b \ll 1. \tag{A8}$$

The linear phenomenological equations, linking a diffusive flux $\tilde{\mathbf{j}}$ to gradients in chemical potential, read

$$\begin{aligned}\tilde{\mathbf{j}}_b &= L_{bb}\nabla\left(\frac{\tilde{\mu}_b'}{m_b} - \frac{\tilde{\mu}_s'}{m_s}\right) + L_{ba}\nabla\left(\frac{\tilde{\mu}_a'}{m_a} - \frac{\tilde{\mu}_s'}{m_s}\right),\\ \tilde{\mathbf{j}}_a &= L_{aa}\nabla\left(\frac{\tilde{\mu}_a'}{m_a} - \frac{\tilde{\mu}_s'}{m_s}\right) + L_{ab}\nabla\left(\frac{\tilde{\mu}_b'}{m_b} - \frac{\tilde{\mu}_s'}{m_s}\right).\end{aligned} \tag{A9}$$

The flux of the solvent can then be calculated from the condition

$$\sum_{i=a,b,s} m_i \tilde{\mathbf{j}}_i = 0. \tag{A10}$$

The coefficients L_{mn} in Eq. (A9) relate gradients in chemical potential to dissipation. For $\tilde{c}_a v_a + \tilde{c}_b v_b \ll 1$, the diagonal coefficients L_{aa} and L_{bb} are proportional to the product of a solute volume fraction and the solvent volume fraction. The solvent volume fraction is close to unity and we set $L_{bb} = -m_b \tilde{c}_b D/kT$ and $L_{aa} = -m_a \tilde{c}_a D/kT$. The cross-coefficents, on the other hand, are proportional to the product of the two solute volume fractions. They obey the Onsager relation $L_{ab} = L_{ba}$. To lowest order in solute volume fractions we therefore have $L_{ab} = L_{ba} \approx 0$ when Eq. (A8) holds. On employing Eqns. (A6-A9) we finally obtain

$$\tilde{\mathbf{j}}_a = -D \nabla \tilde{c}_a, \tag{A11}$$

$$\tilde{\mathbf{j}}_b = -D \left(\nabla \tilde{c}_b + \frac{\tilde{c}_b}{kT} \nabla \tilde{\Psi} \right), \tag{A12}$$

where the surface potential acting on each molecule of type b is defined as $\tilde{\Psi} \equiv v_b \tilde{\Psi}_1$. Due to the assumption of similar specific volumes of the molecules in Eqns. (A6,A7) the pressure becomes a purely hydrodynamic quantity. We have in steady state the common incompressibility condition $\nabla \cdot \tilde{\mathbf{v}} = 0$ since

$$\begin{aligned} 0 =& \nabla \cdot \left[\left(m_a \tilde{c}_a + m_b \tilde{c}_b + m_s \tilde{c}_s \right) \tilde{\mathbf{v}} \right] \approx \\ & \frac{m_s}{v_s} \nabla \cdot \left[\left(\tilde{c}_a v_a + \tilde{c}_b v_b + \tilde{c}_s v_s \right) \tilde{\mathbf{v}} \right] \approx \frac{m_s}{v_s} \nabla \cdot \tilde{\mathbf{v}}. \end{aligned} \tag{A13}$$

Appendix B: Diffusiophoretic swimming for $\lambda \ll 1$

In this Appendix the speed U_0 of active swimmers is calculated analoguous to work by Anderson and Prieve[51] for passive swimmers. The diffusion equation (20,24) becomes in spherical coordinates

$$\begin{aligned} & \partial_r^2 c(r,\theta) + \left(\Psi'(r) + \frac{2}{r} \right) \partial_r c(r,\theta) \\ & + \left(\Psi''(r) + \frac{2}{r} \Psi'(r) \right) c(r,\theta) + \frac{1}{r^2 \sin\theta} \partial_\theta \left(\sin\theta \, \partial_\theta c(r,\theta) \right) \\ & - \frac{\mathrm{Pe}}{\delta} \hat{\mathbf{e}}_r \mathbf{v} \, \partial_r \, e^{-\Psi(r)} = 0. \end{aligned} \tag{B1}$$

Due to the radial symmetry of $\Psi(r)$, only the dipole moment of the concentration field can move the particle. In absence of a coupling between different spherical harmonics it is therefore sufficient to consider the field contributions which are $\sim \cos\theta$. We split the concentration field of type b solute into an inner field $C^i(y)\cos\theta$ and an outer field $C^o(r)\cos\theta$. $C^i(y)$ is written in terms of the inner variable $y \equiv (r-1)/\lambda$. The outer field lies in the region with $r \gg \lambda + 1$ where the effect of the surface potential Ψ is negligible. Eq. (B1) thus becomes here in the outer region

$$\partial_r^2 C^o(r) + \frac{2}{r} \partial_r C^o(r) - \frac{2}{r^2} C^o(r) = 0. \tag{B2}$$

For active diffusiophoresis, the concentration perturbation must vanish far away of the swimmer, Therefore, the solution of Eq. (B2) is $C^o(r) = A/r^2$, where the coefficient A needs to be determined by matching with the far field behavior of C^i. The smallness of λ suggests an expansion of the inner and outer fields as

$$C^i = C_0^i(y) + C_1^i(y)\lambda + C_2^i(y)\lambda^2 + O(\lambda^3), \tag{B3}$$

$$\begin{aligned} C^o = & \frac{1}{r^2} \left(A_0 + A_1 \lambda + A_2 \lambda^2 + \ldots \right) = A_0 + \\ & \left(A_1 - 2A_0 y \right) \lambda + \left(A_2 - 2A_1 y + 3A_0 y^2 \right) \lambda^2 + O(\lambda^3). \end{aligned} \tag{B4}$$

In the inner region we substitute r by $\lambda y + 1$ in Eq. (B1) and expand for small λ. The resulting equations for the two lowest coefficients C_0^i and C_1^i are

$$\partial_y \left(\partial_y C_0^i(y) + C_0^i(y) \partial_y \Psi \right) = 0, \tag{B5}$$

$$\partial_y \left(\partial_y C_1^i(y) + C_1^i(y) \partial_y \Psi \right) + 2 \left(\partial_y C_0^i(y) + C_0^i(y) \partial_y \Psi \right) = 0. \tag{B6}$$

The boundary condition Eqns. (17, 25) yield for the coefficients of $C^i(y)$

$$\frac{-\lambda}{\lambda} \left(\partial_y C_1^i(y) + C_1^i(y) \partial_y \Psi \right) |_{y=0} = \frac{\kappa R}{D\hat{c}} = 1; \tag{B7}$$

$$\frac{-\lambda^n}{\lambda} \left(\partial_y C_n^i(y) + C_n^i(y) \partial_y \Psi \right) |_{y=0} = 0 \qquad \text{when} \quad n \neq 1. \tag{B8}$$

Employing the above equations, the concentration is

$$\begin{aligned} C^i = & e^{-\Psi} a_0 + \lambda \, e^{-\Psi} \left[a_1 - \int_0^y \left(e^{\Psi(y')} - 1 \right) \mathrm{d}y' - y \right] + \\ & O\left(\lambda^2\right). \end{aligned} \tag{B9}$$

The $O(\lambda)$ term diverges for $y \to \infty$. In order to make this divergence explicit, we have removed it from the integral in Eq. (B9) by subtracting 1. The unknown constants in the inner and outer solution are determined by matching them asymptotically[54] through $C_n^o(y \to 0) = C_n^i(y \to \infty)$. The resulting conditions, which must be valid for all y, are

$$A_0 = a_0, \tag{B10}$$

$$A_1 - 2A_0 y = a_1 - \int_0^\infty \left(e^{\Psi(y')} - 1 \right) \mathrm{d}y' - y. \tag{B11}$$

This yields the lowest order coefficients $a_0 = A_0 = 1/2$ and the innermost concentration field is thus given by $C^i \approx \exp(-\Psi)/2$.

In order to calculate the fluid flow near the surface of the swimmer, we employ the Stokes equation (22) and assume that the body force vanishes in the outer region. Applying the curl to Eq. (22) and defining a stream function $S(r)$ via $\mathbf{v} = \nabla \times (\sin\theta S(r)/r\,\hat{\mathbf{e}}_\varphi)$ the Stokes equation becomes

$$\partial_r^4 S(r) - \frac{4\,\partial_r^2 S(r)}{r^2} + \frac{8\,\partial_r S(r)}{r^3} - \frac{8S(r)}{r^4} = -\frac{C^i}{\lambda^2}\,\partial_r \Psi(r). \tag{B12}$$

In the outer region, where the body force vanishes, we have the stream function $S^o = X/r + Y\,r + Z\,r^2$. The constants X,Y and Z are expressed as a power series of λ. The fluid velocity in the outer region thus is

$$\frac{\hat{\mathbf{e}}_\theta \mathbf{v}^o}{\sin\theta} = \frac{-\partial_r S^o(r)}{r} = -2Z_0 - Y_0 + X_0 + O(\lambda), \tag{B13}$$

$$\frac{\hat{\mathbf{e}}_r \mathbf{v}^o}{\cos\theta} = \frac{2S^o(r)}{r^2} = 2Z_0 + 2Y_0 + 2X_0 + O(\lambda). \tag{B14}$$

In the inner region, we expand Eq. (B12) for small λ and insert $C^i(y)$ for the concentration field. The leading order differential equation for the stream function near the surface of the swimmer S^i reads

$$\frac{1}{\lambda}\partial_y^4 S^i(y) = -\frac{e^{-\Psi}}{2}\partial_y \Psi(y). \tag{B15}$$

This yields

$$\begin{aligned} S^i(y) =& k_0 + l_0\,y + m_0\,y^2 + n_0\,y^3 - \frac{\lambda}{2}h(y) \\ & \lambda\left(k_1 + l_1\,y + m_1\,y^2 + n_1\,y^3\right) + O\left(\lambda^2\right); \end{aligned} \tag{B16}$$

$$h(y) \equiv \int_0^y \int_0^{y'} \int_{y''}^\infty \left(e^{-\Psi(y''')} - 1\right) \mathrm{d}y''' \mathrm{d}y'' \mathrm{d}y'. \tag{B17}$$

The fluid flow in the inner region becomes

$$\begin{aligned} &\frac{\hat{\mathbf{e}}_\theta \mathbf{v}^i}{\sin\theta} \approx -\frac{1}{\lambda}\left(l_0 + 2m_0\,y + 3n_0\,y^2\right) + \frac{1}{2}\partial_y h(y) + \\ &\left(-l_1 + l_0 y - 2m_1 y + 2m_0 y^2 - 3n_1 y^2 + 3n_0 y^3\right) + O(\lambda), \end{aligned} \tag{B18}$$

$$\frac{\hat{\mathbf{e}}_r \mathbf{v}^i}{\cos\theta} \approx 2\left(k_0 + l_0\,y + m_0\,y^2 + n_0\,y^3\right) + O(\lambda). \tag{B19}$$

Due to the no slip boundary conditions on the surface of the swimmer we have $k_0 = l_0 = l_1 = 0$. The far field boundary condition on the outer velocity field $\mathbf{v}|_{r\to\infty} = -U\hat{\mathbf{e}}_z$ yields $Z = -U/2$. Matching the lowest order velocities through $\mathbf{v}_n^i(y\to\infty) = \mathbf{v}_n^o(y\to 0)$, as done for the concentrations above, we find

$$0 = -\frac{1}{\lambda}\left(2m_0\,y + 3n_0\,y^2\right), \tag{B20}$$

$$-2Z_0 - Y_0 + X_0 = \frac{K_1}{2} - 2m_1 y + 2m_0 y^2 - 3n_1 y^2 + 3n_0 y^3, \tag{B21}$$

$$2Z_0 + 2Y_0 + 2X_0 = 2m_0\,y^2 + 2n_0\,y^3, \tag{B22}$$

where we have used $\partial_y h(y)|_{y\to\infty} = K_1$ (see Eq. (27)). From Eq. (B20) we deduce that $m_0 = n_0 = 0$. On imposing the physical constraint that $\partial_y h(y)$ remains finite for $y \to \infty$ we conclude that $m_1 = n_1 = 0$ in order to avoid divergence of the right hand side of Eq. (B21). Finally, Eqns. (B21,B22) yield together the two last constants $X_0 = (K_1 - U_0)/4$ and $Y_0 = (3U_0 - K_1)/4$. This fully determines the lowest order velocity fields. To further relate the speed of the swimmer U_0 to the balance of forces, one only needs to consider the Stokeslet $\mathbf{v}^o \sim 1/r$, whose long range nature reflects the presence of external forces. For a free swimmer the Stokeslet vanishes and we therefore have $Y_0 = 0$. This condition determines the lowest order swimming speed

$$U_0 = \frac{K_1}{3}. \tag{B23}$$

The first correction of $O(\lambda^3)$ in a series expansion of $\tilde{U}$ (see Eq. (28)) is an extension of the scheme presented here.

Appendix C: Energy balance in linear, nonequilibrium thermodynamics

This Appendix substantiates the definition of the power input in Sec. VI by providing more details about the underlying assumptions and calculations. As explained in Sec. VI A, we assume that an external apparatus is connected to the system. The apparatus consumes energy and keeps the system in steady state. The ensemble of system and apparatus does not exchange matter but only work and heat with the external world. The first law of thermodynamics for the ensemble reads

$$\tilde{P}_{\mathrm{in}} = \tilde{P}_{\mathrm{out}} + \delta\tilde{Q} \tag{C1}$$

where $\tilde{P}_{\mathrm{out}}$ is the work output of the system. We set $\tilde{P}_{\mathrm{out}} = 0$ because no external force acts on the swimmer. Within the framework of classical, linear, nonequilibrium thermodynamics[55,56], the heat flow $\delta\tilde{Q}$ balances in steady state the entropy production inside the system and the apparatus. We can employ a local definition of the entropy production rate to rewrite the first law

$$\tilde{P}_{\mathrm{in}} = \delta\tilde{Q} = \int T\left(\tilde{\Theta}_{\mathrm{sys}} + \tilde{\Theta}_{\mathrm{app}}\right)\mathrm{d}\tilde{V} \tag{C2}$$

with $\tilde{\Theta}$ being the entropy production rates per unit volume. Since the external apparatus is ideal, we have $\tilde{\Theta}_{\mathrm{app}} = 0$. For the entropy production of the system we employ an established formula[55], which derives from a local equilibrium assumption,

$$\begin{aligned} \tilde{\Theta}_{\mathrm{sys}} =& \frac{1}{T} 2\eta \tilde{E} : (\nabla\tilde{\mathbf{v}}) - \frac{1}{T}\sum_i \tilde{\mathbf{j}}_i \nabla\left(\tilde{\mu}_i + \tilde{\Psi}_i\right) \\ & - \frac{1}{T}\sum_{ki}\left(\tilde{\mu}_i + \tilde{\Psi}_i\right)\tilde{\alpha}_{ik}, \end{aligned} \tag{C3}$$

where $\tilde{\alpha}_{ik}$ is the rate at which the reaction with index k changes the concentration of species i. For the model system considered in Sec. VI, the entropy production rate is rewritten by employing the Stokes equation Eq. (5) and the chemical reactions defined in Eqns. (34,35)

$$T\tilde{\Theta}_{\rm sys} \times \frac{R^2}{kT\hat{c}D} = -\left(\mathbf{j}_b + \mathrm{Pe}\,\mathbf{v}\frac{\tilde{c}_b}{\hat{c}}\right)\nabla\Psi - \sum_i \mathbf{j}_i \nabla\mu_i + \delta\,(r-1)\,g(\theta)\,(\mu_a - \Psi - \mu_b)\,. \tag{C4}$$

In order to calculate $\tilde{P}_{\rm in}$, we assume that the chemical potentials $\tilde{\mu}_a$,$\tilde{\mu}_b$ and $\tilde{\mu}_s$ are fixed by the external apparatus at $\tilde{r} \to \infty$. This, together with Eq. (A6), implies that the concentrations at the outer boundaries of the system are fixed. To facilitate reference, we note here the steady state diffusion equation

$$\nabla \cdot \tilde{\mathbf{J}}_i = \nabla \cdot \left(\tilde{\mathbf{j}}_i + \tilde{\mathbf{v}}\tilde{c}_i\right) = 0. \tag{C5}$$

The solute flux boundary conditions at $\tilde{r} = R$ where $\tilde{\mathbf{v}} = 0$ are given by

$$\begin{aligned} \hat{\mathbf{e}}_r\tilde{\mathbf{j}}_b|_{\tilde{r}=R} &= \frac{D\hat{c}}{R}\,g(\theta), \\ \hat{\mathbf{e}}_r\tilde{\mathbf{j}}_a|_{\tilde{r}=R} &= -\hat{\mathbf{e}}_r\tilde{\mathbf{j}}_b|_{\tilde{r}=R}, \\ \hat{\mathbf{e}}_r\tilde{\mathbf{j}}_s|_{\tilde{r}=R} &= 0. \end{aligned} \tag{C6}$$

Inserting the entropy production rate Eq. (C4) into the expression for the power input Eq. (C2) and using Eq. (C5) for the solute of type b we find

$$\int T\tilde{\Theta}_{\rm sys}\mathrm{d}\tilde{V} = -\int [\nabla\cdot\left[\left(\tilde{\mathbf{j}}_b + \tilde{\mathbf{v}}\tilde{c}_b\right)\tilde{\Psi}\right] + \sum_i \tilde{\mathbf{j}}_i\nabla\tilde{\mu}_i]\,\mathrm{d}\tilde{V} + \int \frac{D\hat{c}}{R}g(\theta)(\tilde{\mu}_a - \tilde{\Psi} - \tilde{\mu}_b)\,\mathrm{d}\tilde{A}_{\tilde{r}=R}. \tag{C7}$$

The potential $\tilde{\Psi}$ now only occurs in surface integrals. $\tilde{\Psi}(\tilde{r})$ decays quickly for $\tilde{r} \to \infty$. Furthermore, using Eq. (C6) leads to a cancelation of surface integrals at $\tilde{r} = R$ containing $\tilde{\Psi}$. We are thus left with

$$\int T\tilde{\Theta}_{\rm sys}\mathrm{d}\tilde{V} = -\int [\tilde{\mathbf{j}}_b\nabla\tilde{\mu}_b + \tilde{\mathbf{j}}_a\nabla\tilde{\mu}_a + \tilde{\mathbf{j}}_s\nabla\tilde{\mu}_s]\,\mathrm{d}\tilde{V} + \int \frac{D\hat{c}}{R}g(\theta)\,(\tilde{\mu}_a - \tilde{\mu}_b)\,\mathrm{d}\tilde{A}_{\tilde{r}=R}. \tag{C8}$$

The Gibbs-Duhem equation, which is consistent with our microscopic model, reads $0 = \sum_i \tilde{c}_i\nabla\tilde{\mu}_i - \nabla\tilde{p}$. Multiplication of this equation by the center of mass flow $\tilde{\mathbf{v}}$ and insertion into Eq.(C8) yields

$$\begin{aligned} \int T\tilde{\Theta}_{\rm sys}\mathrm{d}\tilde{V} &= -\int [\sum_i \left(\tilde{\mathbf{j}}_i + \tilde{\mathbf{v}}\tilde{c}_i\right)\nabla\tilde{\mu}_i - \tilde{\mathbf{v}}\nabla\tilde{p}]\,\mathrm{d}\tilde{V} \\ &\quad + \int \frac{D\hat{c}}{R}g(\theta)\,(\tilde{\mu}_a - \tilde{\mu}_b)\,\mathrm{d}\tilde{A}_{\tilde{r}=R} \\ &= -\int [\sum_i \tilde{\mathbf{J}}_i\tilde{\mu}_i - \tilde{\mathbf{v}}\tilde{p}]\,\hat{\mathbf{e}}_r\mathrm{d}\tilde{A}_{\tilde{r}=\infty} \\ &\quad + \int [\sum_i \hat{\mathbf{e}}_r\tilde{\mathbf{j}}_i\tilde{\mu}_i + \frac{D\hat{c}}{R}g(\theta)\,(\tilde{\mu}_a - \tilde{\mu}_b)]\,\mathrm{d}\tilde{A}_{\tilde{r}=R}, \end{aligned} \tag{C9}$$

where the diffusion equations and $\nabla\cdot\tilde{\mathbf{v}} = 0$ were used to produce the boundary integrals. Due to the boundary conditions Eq. (C6), the last integral in Eq. (C9) vanishes. Since the swimmer is not subjected to external forces, the fluid flow contains no Stokeslet. With the assumptions in Eqns. (A6, A7) the pressure does also not depend on local concentrations. Therefore, the boundary work of the pressure vanishes $\int \tilde{\mathbf{v}}\tilde{p}\,\mathrm{d}\tilde{\mathbf{A}}_{\tilde{r}=\infty} \to 0$ and can consequently be dropped in Eq. (C9). For our model, we conclude that it does not make a difference whether we consider a pressurized system (Gibbs free energy) or a system with fixed volume (free energy). The power input becomes

$$\int T\tilde{\Theta}_{\rm sys}\mathrm{d}\tilde{V} = -\int \sum_i \tilde{\mathbf{J}}_i\tilde{\mu}_i\,\hat{\mathbf{e}}_r\mathrm{d}\tilde{A}_{\tilde{r}=\infty}. \tag{C10}$$

Employing the chemical potentials from Appendix A with the assumption of diluteness ($v_a\tilde{c}_a + v_b\tilde{c}_b \ll 1$) and Eq. (A6) along with Eqns. (C5,C6) we find

$$-\int \sum_{i=a,b,s} \tilde{\mathbf{J}}_i\tilde{\mu}_i\,\hat{\mathbf{e}}_r\mathrm{d}\tilde{A}_{\tilde{r}=\infty} = -\int \sum_{i=a,b} \tilde{\mathbf{J}}_i\tilde{\mu}_i\,\hat{\mathbf{e}}_r\mathrm{d}\tilde{A}_{\tilde{r}=\infty} = \int \tilde{\mathbf{J}}_b\,(kT\log[\tilde{c}_a/\tilde{c}_b] + \epsilon_a - \epsilon_b)\,\hat{\mathbf{e}}_r\mathrm{d}\tilde{A}_{\tilde{r}=\infty}. \tag{C11}$$

This formula is employed in linearized form for Eq. (54).

[1] P. E. Lammert, J. Prost, and R. Bruinsma, J. Theor. Biol. **178**, 387 (1996).
[2] R. Ismagilov, A. Schwartz, N. Bowden, and G. Whitesides, Angew. Chem. Int. Ed. **41**, 652 (2002).
[3] W. F. Paxton, A. Sen, and T. E. Mallouk, Chem. Eur. J. **11** (2005).
[4] R. Golestanian, T. B. Liverpool, and A. Ajdari, Phys. Rev. Lett. **94**, 220801 (2005).
[5] Y. Wang, R. Hernandez, D. Bartlett Jr, J. Bingham, T. Kline, A. Sen, and T. Mallouk, Langmuir **22**, 10451 (2006).
[6] G. Rückner and R. Kapral, Phys.Rev. Lett. **98**, 150603 (2007).
[7] S. Thutupalli, R. Seemann, and S. Herminghaus, New J. Phys. **13**, 073021 (2011).
[8] S. Thakur and R. Kapral, J. Chem. Phys. **135**, 024509 (2011).
[9] G. Ozin, I. Manners, S. Fournier-Bidoz, and A. Arsenault, Adv. Mater. **17**, 3011 (2005).
[10] W. Paxton, S. Sundararajan, T. Mallouk, and A. Sen, Angew. Chem. Int. Ed. **45**, 5420 (2006).
[11] Y. He, J. Wu, and Y. Zhao, Nano Lett. **7**, 1369 (2007).

[12] J. Burdick, R. Laocharoensuk, P. Wheat, J. Posner, and J. Wang, J. Am. Chem. Soc. **130**, 8164 (2008).
[13] D. Kagan, R. Laocharoensuk, M. Zimmerman, C. Clawson, S. Balasubramanian, D. Kagan, D. Bishop, S. Sattayasamitsathit, L. Zhang, and J. Wang, Small **6**, 2741 (2010).
[14] A. Solovev, S. Sanchez, M. Pumera, Y. Mei, and O. Schmidt, Adv. Funct. Mater. **20**, 2430 (2010).
[15] M. Popescu, M. Tasinkevych, and S. Dietrich, Europhys. Lett. **95**, 28004 (2011).
[16] R. Golestanian, Phys. Rev. Lett. **102**, 188305 (2009).
[17] D. Campos and V. Méndez, J. Chem. Phys. **130**, 134711 (2009).
[18] B. ten Hagen, S. van Teeffelen, and H. Löwen, J. Phys.: Condens. Matter **23**, 194119 (2011).
[19] J. Palacci, C. Cottin-Bizonne, C. Ybert, and L. Bocquet, Phys. Rev. Lett. **105**, 88304 (2010).
[20] H. R. Suzuki, R. Jiang and M. Sano, Arxiv preprint arXiv:1104.5607v1(2011).
[21] M. Popescu, S. Dietrich, and G. Oshanin, J. Chem. Phys. **130**, 194702 (2009).
[22] Y. Yang, V. Marceau, and G. Gompper, Phys. Rev. E **82**, 031904 (2010).
[23] M. Enculescu and H. Stark, Phys. Rev. Lett. **107**, 058301 (2011).
[24] S. Thakur, J. Chen, and R. Kapral, Angew. Chem. Int. Ed. **50**, 1 (2011).
[25] S. Hall, E. Khudaish, and A. Hart, Electrochim. acta **43**, 579 (1997).
[26] W. F. Paxton, P. T. Baker, T. R. Kline, Y. Wang, T. E. Mallouk, and A. Sen, J. Am. Chem. Soc. **128**, 14881 (2006).
[27] S. Sundararajan, P. Lammert, A. Zudans, V. Crespi, and A. Sen, Nano Lett. **8**, 1271 (2008).
[28] J. Moran, P. Wheat, and J. Posner, Phys. Rev. E **81**, 065302 (2010).
[29] E. Yariv, Proc. R. Soc. A **467**, 1645 (2011).
[30] J. L. Anderson, Annu. Rev. Fluid Mech. **21**, 61 (1989).
[31] W. F. Paxton, K. C. Kistler, C. C. Olmeda, A. Sen, S. K. St. Angelo, Y. Cao, T. E. Mallouk, P. E. Lammert, and V. H. Crespi, J. Am. Chem. Soc. **126**, 13424 (2004).
[32] J. Gibbs and Y. Zhao, Appl. Phys. Lett. **94**, 163104 (2009).
[33] J. R. Howse, R. A. L. Jones, A. J. Ryan, T. Gough, R. Vafabakhsh, and R. Golestanian, Phys. Rev. Lett. **99**, 48102 (2007).
[34] Y. Shi, L. Huang, and D. Brenner, J. Chem. Phys. **131**, 014705 (2009).
[35] B. Sabass and U. Seifert, Phys. Rev. Lett. **105**, 218103 (2010).
[36] S. Spagnolie and E. Lauga, Phys. Fluids **22**, 031901 (2010).
[37] M. Teubner, J. Chem. Phys. **76**, 5564 (1982).
[38] R. O'Brien and L. White, J. Chem. Soc. Faraday Trans. 2 **74**, 1607 (1978).
[39] J. Happel and H. Brenner, *Low Reynolds number hydrodynamics* (Martinus Nijhoff, 1983).
[40] A. Acrivos and T. D. Taylor, Phys. Fluids **5**, 387 (1962).
[41] H. J. Keh and Y. K. Wei, Langmuir **16**, 5289 (2000).
[42] J. L. Anderson, M. E. Lowell, and D. C. Prieve, J. Fluid Mech. **117** (1982).
[43] D. Saville, Annu. Rev. Fluid Mech. **9**, 321 (1977).
[44] D. Prieve and R. Roman, J. Chem. Soc., Faraday Trans. 2 **83**, 1287 (1987).
[45] J. L. Anderson and D. C. Prieve, Langmuir **7**, 403 (1991).
[46] S. Park and N. Agmon, J. Phys. Chem. B **112**, 12104 (2008).
[47] K. Šolc and W. Stockmayer, J. Chem. Phys. **54**, 2981 (1971).
[48] D. Shoup, G. Lipari, and A. Szabo, Biophys. J. **36**, 697 (1981).
[49] M. J. Lighthill, Commun. Pure Appl. Math. **5** (1952).
[50] H. Ke, S. Ye, R. Carroll, and K. Showalter, J. Phys. Chem. A **114**, 5462 (2010).
[51] J. L. Anderson and D. C. Prieve, Sep. Purif. Methods **13**, 67 (1984).
[52] A. Parmeggiani, F. Jülicher, A. Ajdari, and J. Prost, Phys. Rev. E **60**, 2127 (1999).
[53] A. Ajdari and L. Bocquet, Phys. Rev. Lett. **96**, 186102 (2006).
[54] M. Van Dyke, *Perturbation methods in fluid mechanics* (Parabolic Press, 1975).
[55] S. De Groot and P. Mazur, *Non-equilibrium thermodynamics* (Dover publications, 1984).
[56] F. Jülicher and J. Prost, Eur. Phys. J. E **29**, 27 (2009).